DOKUZ EYLÜL UNIVERSITY

GRADUATE SCHOOL OF NATURAL AND APPLIED SCIENCES

BIOACTIVE COATINGS FOR FUNCTIONALIZATION OF THE MEDICAL IMPLANTS

by

Bensu BAKIN

October, 2015

İZMİR

BIOACTIVE COATINGS FOR FUNCTIONALIZATION OF THE MEDICAL IMPLANTS

A Thesis Submitted to the
Graduate School of Natural and Applied Sciences of Dokuz Eylül University In Partial Fulfillment of the Requirements for the Degree of Master of Science in Metallurgical and Materials Engineering Program

by
Bensu BAKIN

October, 2015
İZMİR

M.Sc THESIS EXAMINATION RESULT FORM

We have read the thesis entitled **"BIOACTIVE COATINGS FOR FUNCTIONALIZATON OF THE MEDICAL IMPLANTS"** completed by **BENSU BAKIN** under supervision of **ASST. PROF. DR. FUNDA AK AZEM** and we certify that in our opinion it is fully adequate, in scope and in quality, as a thesis for the degree of Master of Science.

Asst.Prof.Dr. Funda AK AZEM

Supervisor

Asst.Prof.Dr. Işıl BİRLİK

(Jury Member)

Assoc.Prof.Dr. Osman ÇULHA

(Jury Member)

Prof.Dr. Ayşe OKUR
Director
Graduate School of Natural and Applied Sciences

ACKNOWLEDGMENTS

Firstly, I would like to express to my deep and sincere gratitude to my advisor Assist. Prof. Dr. Funda AK AZEM and co-advisor Assist. Prof. Dr. Işıl BİRLİK, for their excellent guidance, patient supervision and continuous support thought the preparation of this study.

I warmly express my special thanks to my co-workers, Tülay KOÇ DELİCE and Utku TİRİÇ for their supports, helps, patience and friendships. I wish to give my special thanks to my friends İrem ÜNALAN, Mehmet Bulut ÖZYİĞİT, Onur BARDAKÇIOĞLU and Sıdıka YILDIRIM for their valuable friendships and supports. I owe thanks to Aslıhan SÜSLÜ, Çağrı KILINÇ, Güler UNGAN, Haydar KAHRAMAN, Oylum ÇOLPANKAN, Ramazan DALMIŞ and Serhan KÖKTAŞ, for their helps during my experiments.

The present research was also supported by The Scientific and Technological Research Council of Turkey (TÜBİTAK) with project code 112R020 named as; Bioactive coatings for functionalization of the medical implants.

Finally, I would like to express my deep and sincere thanks to my family who always believed in me. I especially thank to Özcan ERSOY for his never-ending support, understanding and encouragement. This thesis work was easier with his presence in my life.

Bensu BAKIN

BIOACTIVE COATINGS FOR FUNCTIONALIZATION OF THE MEDICAL IMPLANTS

ABSTRACT

Titanium (Ti) and its alloys are widely used as implant materials because of excellent mechanical properties and corrosion resistance. However, Ti and its alloys are bioinert. In order to improve the bone bonding ability, titanium is generaly coated with osteoconductive biomaterials such as CaP ceramics. To enhance the biocompability, CaP coating is generally modified by doping with trace amounts of beneficial elements (Mg^{2+}, Sr^{2+}, Na^{+}, K^{+}, F^{-}, Zn^{+2}) which are existed in natural bones. Although the amount of these substitutions is small, they play important roles in the biological activity and interaction between the bone mineral and CaP based implant materials. Several calcium phosphate coating techniques have been used as plasma spraying, biomimetic deposition, sol-gel, and electrochemical deposition. The electrochemical deposition has a variety of advantages such as low process temperature, ability to deposit on porous or complex shape of substrate, low cost and easiness of thickness control. The aim of the study was to investigate the effect of Mg-substitution on corrosion and bioactivity properties of CaP coatings on Ti6Al4V substrates via electrodeposition technique. Chemical and morphological characterizations of the coatings were examined by using X-Ray Diffraction (XRD), Fourier Transform Infrared Spectroscopy (FTIR) and Scanning Electron Microscopy (SEM). Additionally, corrosion properties of the coatings were studied electrochemically by potentiodynamic polarization technique in simulated body fluid (SBF) at 36±1°C and bioactivity properties of the coatings investigated in SBF with varying time 1, 7 and 14 days. In conclusion, Mg-subtitution, while enhancing the bioactivity properties of the coatings, there is no affirmative effect on corrosion properties of the coatings.

Keywords: CaP coatings, bioactivity, electrochemical deposition, Mg substitution, Ti alloys, corrosion

MEDİKAL İMPLANTLARIN İŞLEVSELLEŞTİRİLMESİ İÇİN BİYOAKTİF KAPLAMALAR

ÖZ

Titanyum (Ti) ve alaşımları mükemmel mekanik özellikleri ve korozyon dirençleri nedeniyle implant malzemeleri olarak yaygın bir şekilde kullanılmaktadır. Ancak, Ti ve alaşımları biyoinerttir. Kemik bağlanma kabiliyetini geliştirmek amacıyla titanyum genellikle CaP seramikleri gibi osteokondüktif biyomalzemeler ile kaplanırlar. Biyouyumluluğu artırmak için CaP kaplamalar genellikle doğal kemik yapısında bulunan faydalı elementlerin (Mg^{2+}, Sr^{2+}, Na^{+}, K^{+}, F^{-}, Zn^{+2}) eser miktarda ilave edilmesiyle modifiye edilmektedir. Yeralanların miktarları küçük olmasına rağmen, biyolojik aktivitede ve kemik minerali ile CaP bazlı implant malzemeleri arasındaki etkileşimde önemli bir rol oynamaktadır. Kalsiyum fosfat kaplamalar için, plazma sprey, biyomimetik çöktürme, sol-jel ve elektrokimyasal çöktürme gibi birçok yöntem kullanılmıştır. Elektrokimyasal çöktürme, düşük işlem sıcaklığı, gözenekli yada karmaşık yapıdaki altlıklara çöktürme imkanı sağlaması, düşük maliyeti ve kaplama kalınlığının kolay kontrolü gibi birçok avantaja sahiptir. Çalışmanın amacı Ti6Al4V altlıklar üzerine elektrokimyasal çöktürme tekniği ile kaplanmış CaP kaplamalarda Mg katkısının, korozyon ve biyoaktivite özellikleri üzerindeki etkisini incelemektir. Kaplamaların kimyasal ve morfolojik karakteristikleri X-ışını Difraksiyonu (XRD), Fourier Dönüşümlü Kızılötesi Spektroskopisi (FTIR) ve Taramalı Elektron Mikroskobu (SEM) ile incelenmiştir. İlave olarak kaplamaların korozyon özellikleri vücut benzeri sıvı (SBF) içerisinde 36±1°C'de elektrokimyasal olarak potansiyodinamik polarizasyon tekniği ile ve biyoaktivite özellikleri değişen zamanlarda 1, 7 ve 14 günde vücut benzeri sıvı (SBF) içerisinde incelenmiştir. Sonuç olarak Mg katkısı kaplamaların biyoaktivite özelliklerini geliştirirken korozyon özellikleri üzerinde olumlu bir etkisi olmamıştır.

Anahtar kelimeler: CaP kaplamalar, biyoaktivite, elektrokimyasal çöktürme, Mg katkısı, Ti alaşımları, korozyon

CONTENTS

Page

LIST OF FIGURES

Page

LIST OF TABLES

Page

CHAPTER ONE
INTRODUCTION

Biomaterials are materials used for making devices that can interact with biological systems to coexist for longer service with minimal failure (Mudali, Sridhar, & Raj, 2003). Implants made of titanium and its alloys are widely used in dental and orthopedic fields due to their excellent properties, including high strength-to-weight ratio, low toxicity, and favorable mechanical properties compared to other metals such as stainless steel (Kung, Lee, & Lui, 2010). Unfortunately, titanium and its alloys are bioinert and easily encapsulated after implanting into the living body by fibrous tissue that isolates them from the surrounding bone. Therefore, various surface treatment techniques of Ti and its alloys have been attempted to improve their biocompatibility (Kar, Raja, & Misra, 2006). Calcium phosphate (CaP) ceramics such as dicalcium phosphate dehydrate, monotite, octacalcium phosphate and hydroxyapatite are usually used to coat implant materials in order to make them bioactive. Moreover, calcium phosphate coatings also modify the corrosion behavior of the implant (Drevet, Aaboubi, & Benhayoune, 2012). The substitutions (Na^+, K^+, Mg^{2+}, Fe^{2+}, Zn^{2+}, CO_3^{2-}, $Cl^-$and F^-) in the apatite structure play important roles in the biological activity of both bone mineral and CaP-based implant materials that incorporate element substitutions by influencing porosity, composition and solubility that facilitate bone regeneration (Thian, Huang, Best, Barber, & Bonfield, 2007).

Magnesium (Mg) is one of the essential elements for all living organisms, i.e. 60–65% of total amount of Mg in a human body is found in bones and teeth (Stipniece et al., 2014). Cacciotti et al. (2009), Kolmas et al. (2011) and Kim et al. (2012) reported that presence of Mg incalcified living tissues, suggesting that Mg ions might improve the biocompatibility and bioactivity of CaP ceramics.

There are numerous methods to deposit CaP layers on metallic devices, such as plasma-spraying, magnetron sputtering, electrophoretic methods, sol-gel and electrochemical methods. Electrochemical method, which is an attractive process because highly irregular objects can be coated relatively quickly at low temperatures.

The composition and properties of the coatings can be controlled applied current/voltage, temperature, pH value and the deposition time (Djoˇsic, Pani´C, Stojanovi´C, Mitri´C, & Miˇskovi´C-Stankovi´C, 2012).

The goal of the study was to produce Mg-substituted CaP coatings on Ti6Al4V substrates for enhancing bioactivity and corrosion properties of the coatings.

The structure of the thesis consists of five different parts in addition to this chapter which are summarized below:

Chapter 2 is a literature review, including classification and properties of biomaterials.

Chapter 3 is a literature review, including production methods of CaP coatings.

Chapter 4 is on the experimental work conducted, including substrate preparation, deposition of Mg-substituted CaP coatings, characterization techniques, bioactivity tests and electrochemical measurements.

Chapter 5 presents results and discussions, including XRD, FTIR, SEM, electrochemical measurements results of the Mg-substituted CaP coatings.

Chapter 6 reviews the main conclusions of the study.

CHAPTER TWO
BIOMATERIALS

2.1 Introduction

Biomaterials are widely used in repair, replacement, or augmentation of diseased or damaged parts of the musculoskeletal system such as bones, joints and teeth. A majority of the applications are summarized in Figure 2.1. The main requirement of a biomaterial is that the material and the tissue environment of the body should coexist without having any undesirable or inappropriate effect on each other. Biocompatibility, an essential requirement for any biomaterial, implies the ability of the material to perform effectively with an appropriate host response for the desired application. Common medical devices made of biomaterials include hip replacements, prosthetic heart valves and the less common neurological prostheses and implanted drug delivery systems. These devices when placed inside the body are termed implants when they are intended to remain there for a substantial period of time, and as prosthesis when they are permanently fixed in the body for long-term application till the end of lifetime (Von Recum, 1999).

A biomaterial used to make devices to replace a part or a function of the body in a safe, reliable, economic, and physiologically acceptable manner. A variety of devices and materials is used in the treatment of disease or injury.

The success of a biomaterial or an implant is highly dependent on three major factors: the properties and biocompatibility of the implant, the health condition of the recipient, and the competency of the surgeon who implants and monitors its progress (Park & Lakes, 2007).

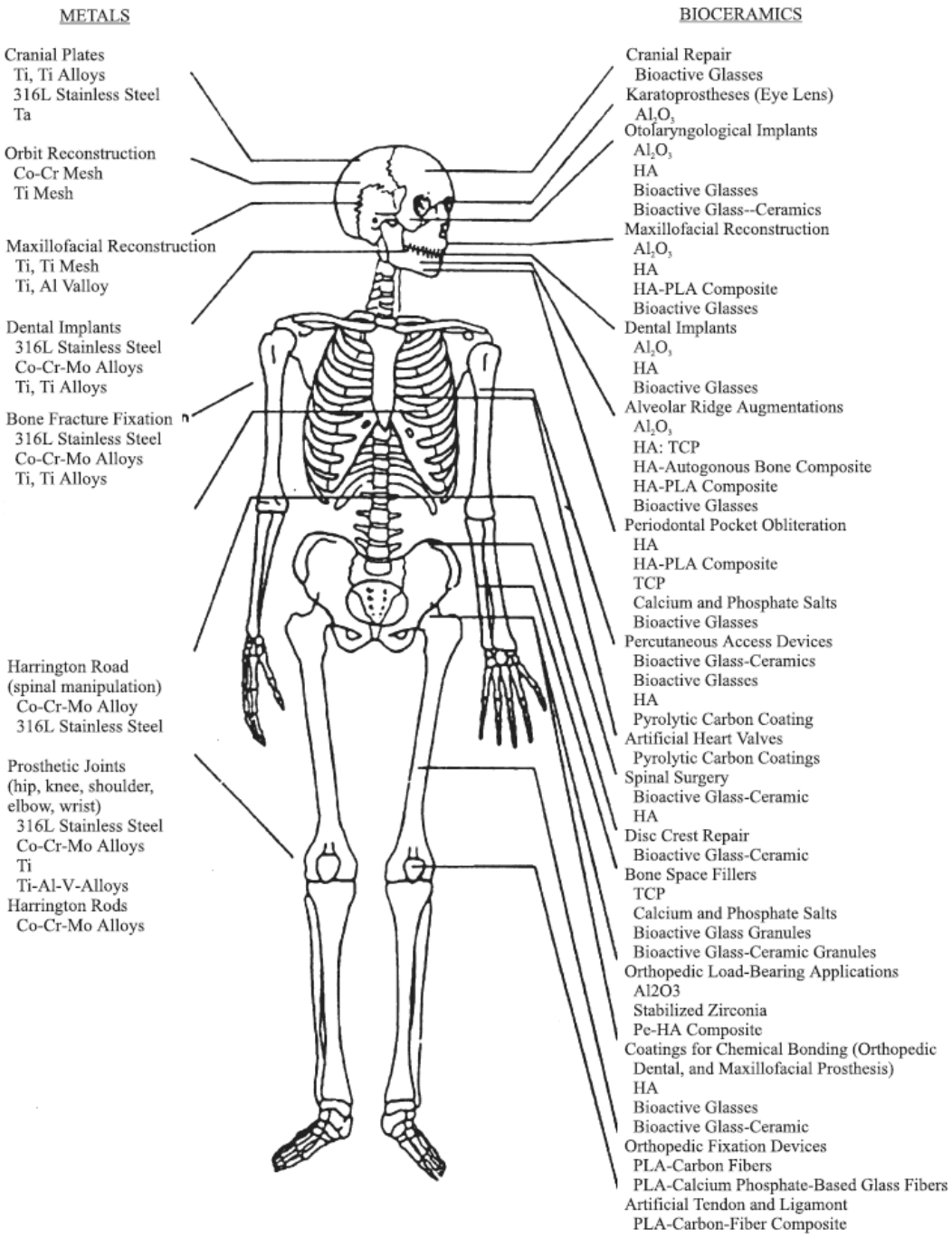

Figure 2.1 Clinical uses of inorganic biomaterials.

Biocompatibility (Figure 2.2) can be defined as, the ability of a material to perform with an appropriate host response in a specific application. This means that the material or any leachable products from it do not cause cell death, chronic inflammation or other impairment of cellular or tissue functions. Implants not only have to be biosafe and biostable in terms of cytotoxicity and degradation, they also

have to match with the biological requirements of any structural biocompatibility. In other words, shape, inner structure and design of an implant need to be adapted to the characteristics of the tissue to be replaced. Besides these bulk requirements, the biocompatibility of surfaces plays a crucial role as the surface is directly exposed to the living organism. Therefore it is necessary to tailor exposed surfaces in view of their chemical, physical, biological and morphological features (Bauer, Schmuki, Klaus von der, & Park, 2013).

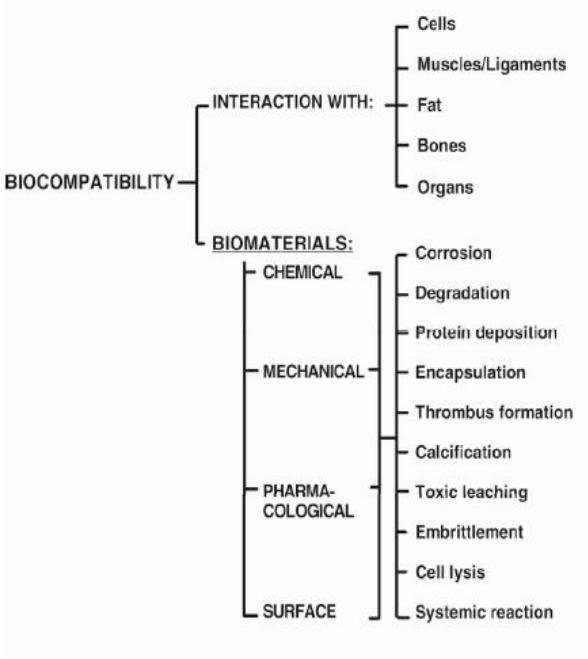

Figure 2.2 Schematic illustration of biocompatibility (Hill, 1998).

Classification of interactions of implants with hard tissue is given in Table 2.1.

Table 2.1 Classification of interactions of implants with hard tissue.

Biocompatible	Release of substances in toxic concentrations that lead to inharmonious effects with the living organism that may result in a rejection of the implant
Biotolerant	Release of substances but not in toxic concentrations that may lead to an encapsulation within connective tissue
Bioinert	No release of toxic substances
Bioactive	Positive interaction with differentiation of tissue that leads to a close adhesion and interconnection along the interface of implant and tissue

The list in Table 2.2 illustrates some of the advantages and disadvantages for three main groups of synthetic (man-made) materials used for implantation.

Table 2.2 General comparison of materials for implants (Park, 1984).

Material Class	Advantages	Disadvantages
Metals	Strong	Corrode in a physiological environment
	Wear resistant	High E
	Tough	High density
	Easy to fabricate	Not usually bioactive
		Not resorbable
Polymers	Resilient	Weak
	Tough	Low E
	Easy to fabricate	Not usually bioactive
	Low density	Nor resorbable
Ceramics	Biocompatible	Low tensile strength
	Wear resistant	Difficult to fabricate
	Lightweight composite	Low toughness
		Not resilient

2.2 Metallic Biomaterials

Metallic materials are most commonly used for load bearing implants and internal fixation devices. Processing method and purity of the metal determines its properties. Some featured properties of a metallic material are its high tensile strength, high yield strength, resistance to cyclic loading (fatigue), resistance to time dependent deformation (creep) and its corrosion resistance. They generally find applications in the fabrication of implant devices such as hip joint prosthesis, knee joint prosthesis, dental implants, cardiovascular devices, surgical instruments, etc.

The first metal alloy developed specifically for human use was the vanadium steel which was used to manufacture bone fracture plates (Sherman plates) and screws. The most commonly used metals and alloys for medical device applications include stainless steels, titanium and its alloys, and cobalt-based alloys (Paital & Dahotre, 2009).

The biocompatibility of the metallic implant is of considerable concern because these implants can corrode in vivo environment (Williams, 1994). The consequences of corrosion are the disintegration of the implant material and the harmful effect of corrosion products on the surrounding tissues and organs.

2.2.1 Stainless Steels

Stainless steels are iron-base alloys with a minimum of 10.5% Cr as an alloying element, needed to prevent the formation of rust. Stainless steel (18Cr–8Ni, type 302, AISI classification) was first used in orthopedic surgery in 1926 (Williams, 1981). For implant applications they must have the resistance to pitting and crevice corrosion from the body plasma.

Although there are several types of stainless steels in use for medical applications, 316L (18Cr–14Ni–2.5Mo) single phase austenitic (FCC) stainless steel is the most popular one for implant applications. The ‘‘L’’ in the designation denotes its low carbon content and as a result it has high corrosion resistance in vivo conditions (Paital & Dahotre, 2009).

The austenitic stainless steels, especially types 316 and 316L, are most widely used for implant fabrication. These cannot be hardened by heat treatment but can be hardened by cold-working. This group of stainless steels is nonmagnetic and possesses better corrosion resistance than any others. The inclusion of molybdenum enhances resistance to pitting corrosion in salt water. The American Society for Testing and Materials (ASTM) recommends type 316L rather than 316 for implant fabrication. According to the ASTM F139-86, specifications for 316L stainless steel are given in Table 2.3. The nickel stabilizes the austenitic phase [γ, face centered cubic crystal (fcc) structure], at room temperature and enhances corrosion resistance.

Table 2.3 Composition of 316L stainless steel (ASTM F139-86).

Element	**Composition (%)**
Carbon	0.03 max
Manganese	2.00 max
Phosphorous	0.03 max
Sulfur	0.03 max
Silicon	0.75 max
Chromium	17.00-20.00
Nickel	12.00-14.00
Molybdenum	2.00-4.00

Today, stainless steel is one of the most frequently used biomaterials for internal fixation devices because of a favorable combination of mechanical properties, corrosion resistance and cost effectiveness when compared to other metallic implants (Disegi, & Eschbach, 2000). Even the 316L stainless steels may corrode inside the body under certain circumstances in a highly stressed and oxygen depleted region, such as the contacts under the screws of the bone fracture plate. Thus, these stainless steels are suit for use only in temporary implant devices such as fracture plates, screws, and hip nails.

2.2.2 Cobalt Alloys

Co–Cr-based alloys are the most commonly used representative Co alloys for biomedical applications. The presence of Cr imparts the corrosion resistance and the addition of small amounts of other elements such as iron, molybdenum, or tungsten can give very good high temperature properties and abrasion resistance (Williams, 1981).

The various types of Co–Cr alloys used for implant applications include Co–Cr–Mo (ASTM F75), Co–Cr–Mo (ASTM F1537), Co–Cr–W–Ni (ASTM F90) and Co–Ni–Cr–Mo–Ti (ASTM F562) (Ratner, Hoffman, Schoen, & Lemons, 2004). Clinical applications of such alloys include its use in dentistry and maxillofacial surgery as (a) partial denture, (b) dental implants, and (c) maxillofacial implants and in

orthopedics as (a) fracture fixation plates and screws and (b) hip and knee prosthesis (Williams, 1981).

Chemical compositions of Co-based alloys are given in Table 2.4.

Table 2.4 Chemical compositions of Co-based alloys (ASTM, 2000) (Park & Lakes, 2007).

	Co28Cr6Mo (F75) Castable		**Co20Cr15W10Ni (F90) Wrought**		**Co28Cr6Mo (F1537) Wrought**		**Co35Ni20Cr10Mo (F562)**	
Element	**Min.**	**Max.**	**Min.**	**Max.**	**Min.**	**Max.**	**Min.**	**Max.**
Cr	27.0	30.00	19.00	21.00	26.0	30.0	19.0	21.0
Mo	5.0	7.00	-	-	5.0	7.0	9.0	10.5
Ni	-	2.5	9.00	11.00	-	1.0	33.0	37.0
Fe	-	0.75	-	3.00	-	0.75	9.0	10.5
C	-	0.35	0.05	0.15	-	0.35	-	0.025
Si	-	1.00	-	1.00	-	1.0	-	0.15
Mn	-	1.00	-	2.00	-	1.0	-	0.15
W	-	0.20	14.00	16.00	-	-		
P	-	0.020	-	0.040	-	-	-	0.015
S	-	0.010	-	0.030	-	-	-	0.010
N	-	0.25	-	-	-	0.25	-	-
Al	-	0.30	-	-	-	-	-	-
Bo	-	0.01	-	-	-	-	-	0.015
Ti							-	1.0
Co				Balance				

2.2.3 Titanium and Titanium Alloys

Titanium's lightness (4.5 g/cm^3) and good mechanochemical properties are remarkable features for implant application (Dowson, 1992). Bothe, Beaton, and Davenport implanted titanium into laboratory animals first time in 1940 (Williams, 1981) and they concluded that titanium as a well-tolerated material under in vivo conditions as compared to stainless steel and Co–Cr based alloys.

The two most commercially used specifications for implants are pure Ti (ASTM F67) and Ti–6Al–4V (ASTM F136) (Ratner, Hoffman, Schoen, & Lemons, 2004).

These alloys have driven a lot of interest for load bearing implants due to its superior mechanical properties (tensile strength and fatigue strength), chemical stability (corrosion resistance), and biocompatibility under in vivo conditions. Commercially pure Ti is selected for applications where corrosion resistance is of prime importance than its mechanical properties. Ti–6Al–4V (ASTM F136) is an alpha–beta alloy, mechanical behavior and chemical stability of which depend upon the type of heat treatment and mechanical working (Black, 1988). Mechanical properties and the clinical applications of Ti alloys listed in Table 2.5

Table 2.5 Mechanical properties and clinical applications of Ti-based materials (Paital & Dahotre, 2009).

Alloy designation	**Elastic modulus (GPa)**	**Ultimate tensile strength (MPa)**	**Elongation (%)**	**Clinical applications**
Pure Ti (ASTM F67)	102-110	240-550	15-24	Pace maker cases, housings for ventricular-assist devices, implantable influsion drug pumps, dental implants, screws and staples for spinal surgery
Ti-6Al-4V (ASTM F136)	110	930	10-15	Total joint replacement arthroplasty primarily for hips and knees
Ti-6Al-7Nb (ASTM F1295)	105	860	10	Femoral hip stems, fracture fixation plates,spinal components, nails, rods, screws and wires
Ti-13Nb-13Zr (ASTM F1713)	79-84	973-1037	10-16	Orthopedic implants

2.3 Polymeric Biomaterials

Polymers are long chain molecules consisting of large number of small repeating units known as monomers. They belong to the family of macromolecules and

represent the largest class of biomaterials. Polymers can be derived either from natural sources or from synthetic organic sources (Paital & Dahotre, 2009).

Synthetic polymeric materials have been widely used in medical disposable supplies, prosthetic materials, dental materials, implants, dressings, extracorporeal devices, encapsulants, polymeric drug delivery systems, tissue engineered products, and orthodoses like those of metal and ceramics substituents. The required properties of polymeric biomaterials are similar to other biomaterials, that is, biocompatibility, sterilizability, adequate mechanical and physical properties, and manufacturability as given in Table 2.6 (Lee, Khang, & Lee, 2003).

Table 2.6 Requirements for biomedical polymers.

Property	Description
Biocompatibility	Noncarcinogenesisi, nonpyrogenicity, nontoxicity, and nonallergic response
Sterilizability	Autoclave, dry heating, ethylenoxide, gas, and radiation
Physical property	Strength, elasticity, and durability
Manufacturability	Machining, molding, extruding and fiber forming

Some advantages associated with polymers, for use as biomaterials can be listed as follows:

- Polymers can be easily fabricated to various complex shapes and structures.
- Provide wide range of bulk compositions and physical properties.
- Surface properties can be easily tuned.

On the other hand their disadvantages include:

- Difficulty in sterilization.
- Easily absorb water and biomolecule from the surroundings and thereby alter the surface chemistry.
- Being soft materials may undergo mechanical wear and breakdown.

- May leach some harmful compounds to the body under in vivo conditions (Paital & Dahotre, 2009).

2.4 Ceramic Biomaterials

Ceramics are inorganic compounds of metallic or nonmetallic materials, with interatomic bonding as ionic or covalent and which are generally formed at elevated temperatures.

A class of such materials used for skeletal or hard tissue repair are commonly referred to bioceramics. These bioceramics may be bioinert (alumina, zirconia), bioresorbable (tricalcium phosphate), bioactive (hydroxyapatite, bioactive glasses, and glass ceramics), or porous for tissue in growth (hydroxyapatite coating, and bioglass coating on metallic materials) (Paital & Dahotre, 2009). Their success depends on their ability to induce bone regeneration and bone in growth at the tissue–implant interface without the intermediate fibrous tissue layer. Desired properties of implanted bioceramics are listed as follows:

- Should be nontoxic
- Should be noncarcinogenic
- Should be nonallergic
- Should be noninflammatory
- Should be biocompatible
- Should be biofunctional for its lifetime in the host.

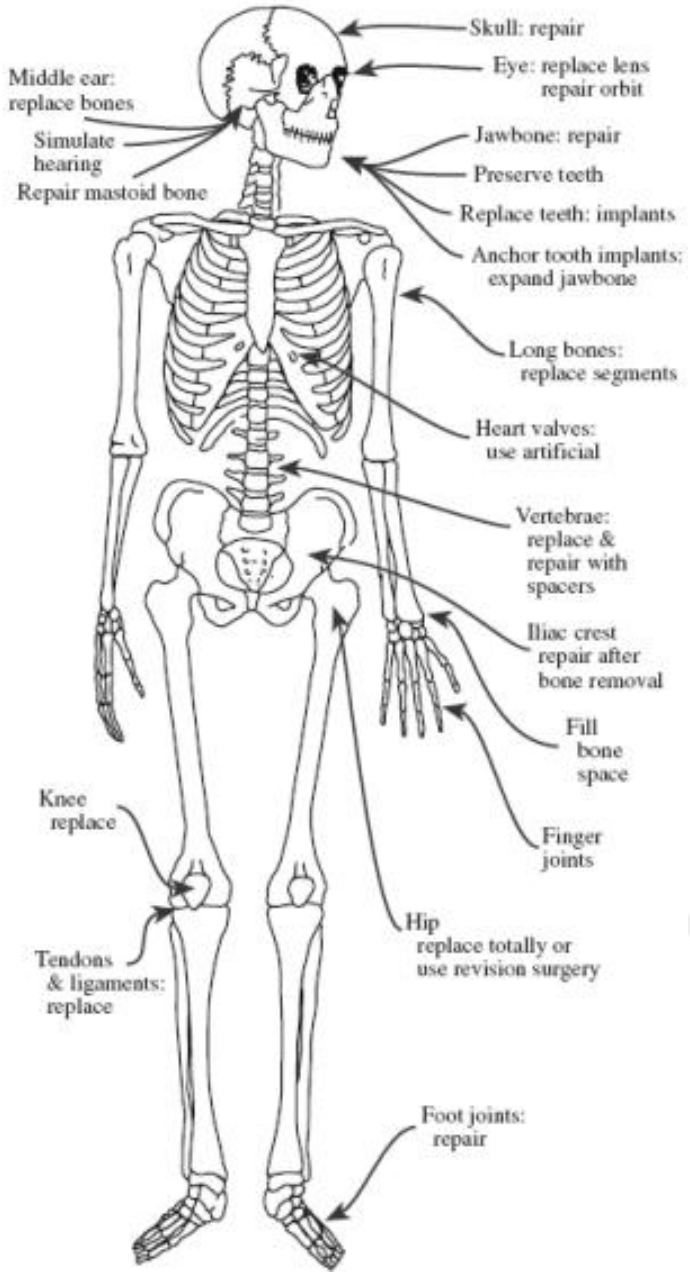

Figure 2.3 Illustration of the head-to-toe clinical uses for bioceramic (Hench, 1991).

Classification of the bioceramics is given in Table 2.7.

Table 2.7 Types of bioceramic tissue attachments (Hench, 1998).

Types of attachment	Types of bioceramic
Dense, nonporous, almost inert ceramics attach by bone growth into surface irregularities by cementing the device into the tissue, or by press-fitting into a defect (morphological fixation)	Al_2O_3 ZrO_2
For porous implants, bone ingrowth occurs, which mechanically attaches the bone to the material (biological fixation)	Porous hydroxyapatite Hydroxyapatite-coated porous metals
Surface-reactive ceramics, glasses, and glass-ceramics attach directly by chemical bonding with the bone (bioactive fixation)	Bioactive glass-ceramics Dense hydroxyapatite Bioactive glasses
Resorbable ceramics and glasses in bulk or powder form designed to be slowly replaced by bone	Calcium sulfate (plaster of Paris) Tricalcium phosphate Calcium phosphate salts Bioactive glasses

2.4.1 Nonabsorbable or Relatively Bioinert Bioceramics

Relatively bioinert ceramics maintain their physical and mechanical properties while in the host enviroment. They resist corrosion and wear and have all the properties listed for desired of bioceramics. Examples of relatively bioinert ceramics are dense and porous aluminum oxides, zirconia ceramics, and single-phase calcium aluminates. Relatively bioinert ceramics are typically used as structural-support implants. Some of these are bone plates, bone screws, and femoral heads. Examples of nonstructural support uses are ventilation tubes, sterilization devices and drug delivery devices (Feenstra & de Groot, 1983).

2.4.1.1 Alumina (Al_2O_3)

The main source of high purity alumina (aluminum oxide, Al_2O_3) is bauxite and native corundum. The commonly available alumina (alpha, α) can be prepared by calcining alumina trihydrate. The American Society for Testing and Materials (ASTM) specifies that alumina for implant use should contain 99.5% pure alumina and less than 0.1% combined SiO_2 and alkali oxides (mostly Na_2O) (F603-78).

In orthopedics area, aluminum oxide has been used for more than 25 years. Alumina is usually a quite hard material; its hardness varies from 20 to 30 GPa. Both polycrystalline and single-crystal alumina have been used clinically. The high hardness is accompanied by low friction and wear and inertness to the in vivo environment. These properties make alumina an ideal material for use in joint replacements (Billotte, 2003).

Graves et al. (1972), implanted aluminum oxide implants in bones of rhesus monkeys and they have shown no signs of rejection or toxicity for 350 days. One of the most popular uses for aluminum oxide is in total hip prostheses. Oonishi (1992), have been claimed that aluminum oxide hip prostheses with an ultra-high-molecular-weight polyethylene (UHMWPE) socket to be a better device than a metal prosthesis with a UHMWPE socket.

2.4.1.2 Zirconia

Pure zirconia can be obtained from chemical conversion of zircon ($ZrSiO_4$), which is an abundant mineral deposit (Billotte, 2003).

Zirconia (ZrO_2) have been tried for application in fabricating implants. Some mechanical properties are as good or better than alumina ceramics. Zirconia is highly biocompatible, as are other ceramics, and can be made in the form of large implants such as the femoral head and acetabular cup in total hip joint replacement (Park & Lakes, 2007).

2.4.2 Calcium Phosphate Ceramics

Biologically relevant CaP belong to the orthophosphate group and naturally occur in several biological structures, including teeth and bone. Bone consists of an inorganic component of biological apatites (CaP) and an organic component, consisting primarily of collagen and water.

Recently, this material has been synthesized and used for manufacturing various forms of implant as well as for solid or porous coatings on other implants. There are mono-, di-, tri-, and tetra-calcium phosphates, in addition to the hydroxyapatite and β-whitlockite, which have ratios of 5/3 and 3/2 for calcium and phosphorus (Ca/P), respectively. The stability in solution generally increases with increasing Ca/P ratios (Park & Lakes, 2007).

Table 2.8 summarizes the calcium phosphate phases, and a brief review of their properties follows below.

Table 2.8 Chemical names, formulas, and Ca/P ratios of various Ca–P based ceramics (Paital & Dahotre, 2009)

Name	Abbrevation	Formula	Ca/P ratio
Calcium phosphate dihydrate (brushite)	DCP	$CaHPO_4.2H_2O$	1.0
Anhydrous calcium phosphate (monetite)	ADCP	$CaHPO_4$	1.0
Octacalcium phosphate	OCP	$Ca_8H_2(PO_4)_6.5H_2O$	1.33
Tricalcium phosphate (whitlockite)	TCP	$Ca_3(PO_4)_2$	1.5
Fluorapatite	FA	$Ca_{10}(PO_4)_6.F_2$	1.67
Hydroxyapatite	HAP	$Ca_{10}(PO_4)_6(OH)_2$	1.6
Tetracalcium phosphate (hilgenstockite)	TTCP	$CaO.Ca_3(PO4)_2$	2.0

2.4.2.1 Calcium Phosphate Dihydrate – Brushite (DCP)

DCP crystals are monoclinic and exhibit greater solubility than most other calcium phosphate phases. It is a precursor to the more stable phase hydroxyapatite (HAP). In environments with a pH greater than 6–7, brushite becomes unstable and transforms to the more favourable HAP phase. Prior investigations have also utilized the increased solubility of DCP on metallic implants as a means of increasing the amounts of calcium and phosphate ions available in the immediate vicinity of the implant to promote increased osseointegration (Kumar, Dasarathy, & Riley, 1999). DCP is also often used as the preliminary component of bone cements in the clinical field (Barrëre, van Blitterswijk & de Groot, 2006). Biocompatibility of this phase has also been shown in vivo in sheep, where effective resorption was illustrated in a cranial defect site (Kuemmerle et al., 2005) and new bone formation was observed in the absence of inflammation (Theiss et al., 2005).

2.4.2.2 Anhydrous Calcium Phosphate – Monetite (ADCP)

ADCP crystals are triclinic and stable at higher temperatures and lower pH levels in the range of pH 4–5. ADCP have also been shown experimentally (Fujishiro, Yabuki, Kawamura, Sato, Okuwaki, 1993; Stulajterov & Medveck, 2008) to undergo conversion from the unstable states at pH levels greater than 6–7 to the more thermodynamically favourable HAP. As mentioned previously, the increased release of calcium and phosphate ions can be advantageous as it promotes osseointegration and osteogenesis. Current studies have demonstrated the adherence, spread and differentiation of human osteoblast cells on three-dimensional (3-D) printed ADCP substrates after periods of 14 and 21 days in culture (Suwanprateeb, Suvannapruk, & Wasoontararat, 2010). In vivo investigations have involved the implantation of ADCP bone cements in the femoral region of rabbits, where biocompatibility and osteoconductivity were observed 3 weeks postoperatively (Khairoun et al., 2002).

2.4.2.3 Octacalcium Phosphate (OCP)

OCP crystals are structurally triclinic crystals and exist in alternating layers of apatite layers and hydrated layers. OCP is often observed as an intermediary stage in the precipitation of HAP and bone-like apatites. It has been suggested and demonstrated experimentally that HAP is unable to be formed directly from solution and thus requires an intermediary phase, most often indicated to be OCP (Suzuki, Imaizumi, Kamakura, & Katagiri, 2008). Barrëre et al. (2001), Barrëre et al. (2003) and Habibovic et al. (2005) reported that OCP to be most stable at a physiological pH and temperature, and have demonstrated the ability of OCP to convert to a bone-like apatite when exposed to slightly more acidic conditions (Reiner & Gotman, 2010). Furthermore OCP has been established as a precursor for bone mineralization. In vitro studies have demonstrated OCP to have excellent biocompatibility.

2.4.2.4 Tricalcium Phosphate – Whitlockite (TCP)

TCP, known mineralogically as whitlockite, commonly exists in two phases: α-TCP and β-TCP. Tricalcium phosphate is often investigated as a biphasic coating in combination with HAP, where studies have indicated that the most effective combinations for increased biocompatibility consist of higher HAP:TCP ratios (Yamada, Heymann, Bouler, & Daculsi, 1997). Clinically, TCP/HAP coatings have demonstrated increased biocompatibility and decreased bone loss when applied to titanium hip implants 2 years postoperatively compared to non-coated implants (Tanzer, Kantor, Rosenthall, & Bobyn, 2001).

2.4.2.5 Hydroxyapatite (HAP)

HAP was the first calcium phosphate product that became commercially available and was used in dentistry and medicine in dense and porous forms. The dissolution rates of some of these materials under simulated physiological conditions have been investigated with emphasis placed on hydroxyapatite, β-tricalcium phosphate and

tetra-calcium phosphate. Under in vitro conditions, the solubility of these materials has been shown to decrease in order of (Klein, Driessens, & de Groot, 1984).

Tetra-calcium phosphate > β-tricalcium phosphate > Hydroxyapatite

Hydroxyapatite is the most important among the calcium compounds since it is found in natural hard tissues as mineral phase. The mineral part of teeth and bones is made of an apatite of calcium and phosphorus similar to HAP ($Ca_{10}(PO_4)_6(OH)_2$) crystals. Natural bone is 70% HAP by weight and 50% HAP by volume. Synthetic, stoichiometric HAP has the formula $Ca_{10}(PO_4)_6(OH)_2$ and belongs to a broad group of calcium-containing minerals based around the phosphate (PO_4^{3-}) group and is characterized by a calcium/phosphorus (Ca/P) molar ratio of 1.67 and the calculated density is 3.219 g/cm^3 (Ak Azem, 2008). HAP has been synthesized and used to manufacture various forms of implants (solid and porous) and as a coating on other implants. Chemical and physical data for HAP is given in Table 2.9 and structure of HAP is given Figure 2.4.

Table 2.9 Chemical and physical data for HAP.

Lattice parameter (Å)	a= 9.432 c=6.8810
Bravais lattice	Hexagonal
Coefficient of thermal expansion (10^{-6} x W/m/K)	13.3
Solubility product Ksp	2.34 x 10^{-59}
Density (g/cm^3)	3.156
Thermal conductivity (W/m/K)	0.72

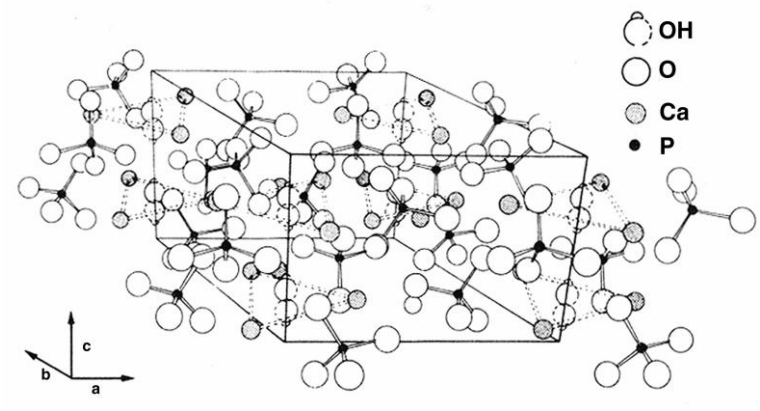

Figure 2.4 The structure of hydroxyapatite.

Among the most important properties of hydroxyapatite as a biomaterial is its excellent biocompatibility. Hydroxyapatite appears to form a direct chemical bond with hard tissues. On implantation of hydroxyapatite particles or porous blocks in bone, new lamellar cancellous bone forms within 4 to 8 weeks (Bajpai & Fuchs, 1985).

However, synthetic HAP differs in composition from bone mineral, as, in addition to calcium, phosphorus, oxygen, and hydrogen ions, bone mineral contains a number of ionic substitutions in its lattice and can also be non-stoichiometric with Ca/P≠1.67 (Ak Azem, 2008).

Substitutions in the HAP structure are possible. Na^{+}, K^{+}, Mg^{2+}, Fe^{2+}, Zn^{2+}, CO_3^{2-}, $Cl^{-}$and F^{-} are the main ion substitutes ions and they differ in variety and amount depending on many factors, such as genetic, individual characteristics and internal environment of the mineralized structures (Thian, Huang, Best, Barber, & Bonfield, 2007).

Mg is one of the essential elements for all living organisms, i.e. 60–65% of total amount of Mg in a human body is found in bones and teeth, and the remaining 35–40% of Mg are scattered throughout the rest of the body (Stipniece et al., 2014). Cacciotti et al. (2009) , Kolmas et al. (2011) and Kim et al. (2012) reported that presence of Mg incalcified living tissues, suggesting that Mg ions might improve the

biocompatibility and bioactivity of CaP ceramics. Magnesium deficiency adversely affects all stages of skeletal metabolism, causing cessation of bone growth, decrease of osteoblastic and osteoclastic activities, osteopenia and bone fragility (Landi et al., 2008).

2.4.3 Bioactive Glass Ceramics

Glass-ceramics are polycrystalline ceramics made by controlled crystallization of glasses. They were originally developed by S.D. Stookey of Corning Glass Works in the early 1960s. They were first utilized in photosensitive glasses in which small amounts of copper, silver and gold are precipitated by ultraviolet light irradiation. These metallic precipitates help to nucleate and crystallize the glass into a fine grained ceramic which possess excellent mechanical and thermal properties. Bioglass® and Ceravital® are two glass-ceramics developed for implants (Park & Lakes, 2007). The composition of Ceravital® is similar to the Bioglass® in terms of SiO_2 content but differs somewhat in others, as given in Table 2.10.

Table 2.10 Compositions of Bioglass® and Ceravital® Glass-Ceramics.

Type	**Code**	**SiO_2**	**CaO**	**Na_2O**	**P_2O_5**	**MgO**	**K_2O**
Bioglass	42S5.6	42.1	29.0	26.3	2.6	–	–
	(45S5)46S5.2	46.1	26.9	24.4	2.6	–	–
	49S4.9	49.1	25.3	23.0	2.6	–	–
	52S4.6	52.1	23.8	21.5	2.6	–	–
Cervital*	Bioactive	40.0–50.0	30.0–35.0	5.0–10.0	10.0–15.0	2.5–5.0	0.5-3.0
	**Nonbioactive	30.0–35.0	25.0–30.0	3.5–7.5	7.5–12.0	1.0–2.5	0.5–2.0

*The Ceravital composition is in weight % while the Bioglass compositions are in mol %.

**In addition Al_2O_3(5.0–15.0), TiO_2 (1.0–5.0) and Ta_2O_5 (5.0–15.0) are added.

A negative characteristic of the glass ceramic is its brittleness. In addition, limitations on the compositions used for producing a biocompatibile (or osteoconductive) glass ceramic hinders the production of a glass ceramic which has substantially higher mechanical strength. Thus, glass ceramics cannot be used for making major load-bearing implants such as joint implants. However, they can be used as fillers for bone cement, dental restorative composites, and coating material (Billotte, 2003) .

CHAPTER THREE
PRODUCTION OF CaP COATINGS

3.1 Plasma Spraying

Plasma spraying is a technique in which a so-called plasma gun creates an electric arc current of high energy between a cathode and an anode. An inert gas is directed through the space between these electrodes, and subsequently the arc current ionizes the gas, and a plasma is formed. Typically used plasma gasses are He, Ar, N_2, H_2 and mixture of these gasses. Argon is usually chosen as the base gas as it ionizes easily and also provides a stable arc at very low operating voltage (Brunette, Tengvall, Textor, & Thomsen, 2001).

The temperature at the core region of plasma exceeds 30.000 K. The electrons and ions in this plasma are separated from each other and are accelerated toward the cathode and anode, respectively. These rapidly moving particles then collide with other atoms or molecules in the gas, which results in expansion owing to the temperature increase. Then, a plasma flame is formed that emerges from the gun toward the substrate at velocities approaching or exceeding the speed of sound. Next, ceramic powder particles are fed into the plasma flame. The particles melt and are deposited on the substrate at which the gun is aimed. The quality of plasma spray-deposited coatings can be influenced by several parameters, such as the temperature of the plasma, the nature of the plasma gas, the particle size of the powder, and the chemical nature of the ceramic powder (Leon & Jansen, 2009).

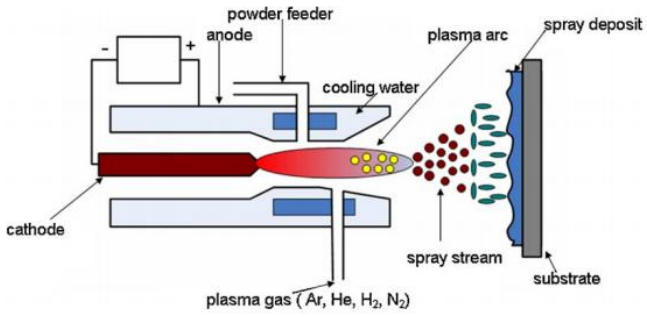

Figure 3.1 Schematic setup of an arc plasma system.

In the past decades, several coating methods have been developed to deposit HAP onto titanium surface, including plasma spraying, ion beam sputtering, sol-gel, electrophoretic deposition, and electrochemical deposition, etc. Among these methods, plasma spraying is the most popular method for coating on titanium implant surfaces. However, the high temperature of the plasma spray usually generates the decomposition of the HAP. Moreover, plasma spray coating technique is not capable of producing a uniform HAP coating on implant with a complex shape and plasma sprayed HAP has a disadvantage of possessing low bonding strength at coatings/implant interface (Isa, Mohd, & Yury, 2012).

3.2 Magnetron Sputtering

Magnetron sputtering has developed rapidly over the last decade to the point where it has become established as the process of choice for the deposition of a wide range of industrially important coatings. The driving force behind this development has been the increasing demand for high-quality functional films in many diverse market sectors. In many cases, magnetron sputtered films now outperform films deposited by other physical vapour deposition (PVD) processes, and can offer the same functionality as much thicker films produced by other surface coating techniques. Consequently, magnetron sputtering now makes a signifcant impact in application areas including hard, wear-resistant coatings, low friction coatings, corrosion-resistant coatings, decorative coatings and coatings with specific optical, or electrical properties (Kelly & Arnell, 2000).

Sputtering in general is a process where atoms or molecules are ejected from the target by the bombardment of high-energy particles. Material is ejected from the target in a way to obtain usable quantities of material which can be directly deposited onto the substrate. For effective coating using sputtering process two important criteria must be met:

- ions of sufficient energy must be created and directed towards the surface of the target to eject atoms from the material

- the ejected atoms must be able to move freely towards the object to be coated with little impedance to their movement (Paital & Dahotre, 2009).

However, the process is limited by low deposition rates, low ionisation efficiencies in the plasma, and high substrate heating efects. These limitations have been overcome by the development of magnetron sputtering (Kelly & Arnell, 2000).

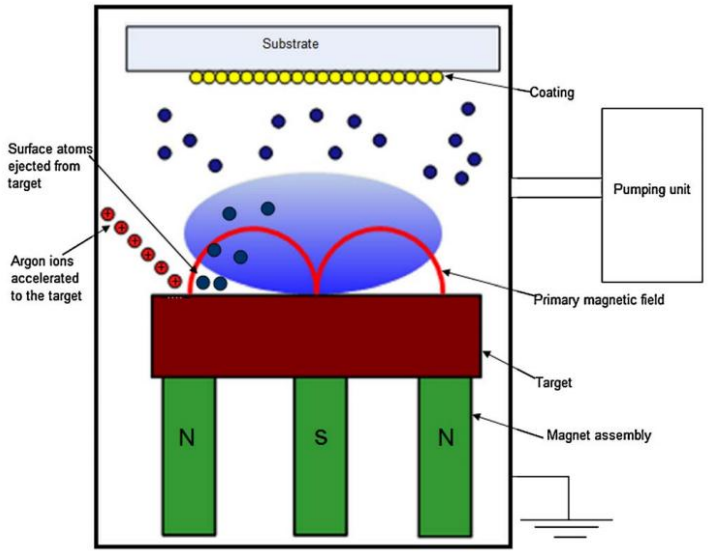

Figure 3.2 Schematic of a magnetron sputter deposition system.

The main advantages of magnetron sputtering are as follows:

- low plasma impedance and thus high discharge currents from
- deposition rates in the range from 1 nm/s to 10 nm/s
- low thermal load to the substrate
- coating uniformity in the range of a few percent even for several meters long cathodes
- easy to scale up
- dense and well adherent coatings
- large variety of film materials available (nearly all metals and compounds) (Brauer, Szyszka, Vergohl, & Bandorf, 2010).

Many researchers have explored the deposition of CaP films on metallic materials for implant applications by this technique. Apart from its favorable mechanical properties and in vitro biocompatibility, CaP coatings obtained using this technique also proved for its strong in vivo response by inducing bone growth at the interface. Based on the results the authors demonstrated the efficacy of magnetron sputtering technique to synthesize CaP coatings for load bearing implants (Paital & Dahotre, 2009).

3.3 Sol–gel Derived Coatings

Sol–gel technique has been well developed and employed to prepare various materials because the technique has the main advantages of the easy control of chemical composition and low temperature synthesis that are very important for film preparation. Production of CaP coatings by using sol-gel technique received more attention over the past 10 years because of its advantages (Weng et al., 2003).

Sol–gel processing can be broadly defined by a series of experimental steps as mentioned below:

- At the first step it involves the preparation of a sol, generally by the in situ generation of ultrafine particles in a liquid vehicle. This is mostly due to the hydrolysis and condensation reactions occurring when a metal alkoxide is mixed with water and a mutual solvent (mostly alcohol) in the presence of acid or base catalyst (via growth of polymeric molecules or Ostwald ripening).
- This is followed by ageing of the sol at a suitable temperature for arriving at desired properties (e.g., optimum viscosity).
- The sol is then subjected to casting, spinning, drawing, coating, emulsification, dipping, spraying, etc. for obtaining the required gel form coating through sol–gel transition.
- At the final stage the specimen is subjected to drying, followed by heating in most cases to obtain the desired product.

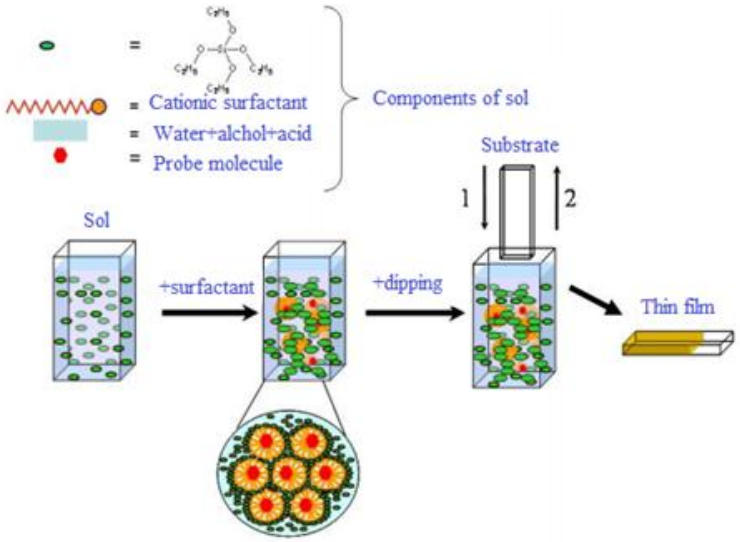

Figure 3.3 Flow chart of sol-gel process.

Brinker and Scherer (1990), have broadly divided these parameters into two categories: the respected and the neglected ones. Respected parameters are important specially in defining the quality of the sol, and consequently, that of the corresponding gel. On the other hand, the neglected parameters probably demand lesser attention, but may affect the properties of the sol and the gel when neglected completely. These parameters are given in Table 3.1.

Table 3.1 Various parameters in sol–gel processing.

Some Respected Parameters	**Some Neglected Parameters**
Choice of precursors	Volatile evolution rate in sol
Concentration of Precursors (i.e. addition of water, organics)	Variations in ambient conditions
Type and amount of catalyst	Rate of change of viscosity etc.
Control of hydrolysis reaction etc.	

Some advantages associated with sol–gel coating technique can be listed as follows:

- It can produce thin bond-coating to provide excellent adhesion between the metallic substrate and the top coat.

- Can easily shape materials into complex geometries in a gel state.
- It can produce high-purity products as the organo-metallic precursor of the desired ceramic oxides can be mixed, dissolved in a specified solvent and hydrolyzed into a sol, and subsequentlya gel. Hence, the composition can be highly controlled.
- Provides an excellent matrix for entrapping a variety of organic and inorganic compounds and biologically important molecules.
- Possesses low temperature sintering capability, usually 200–600˚ C.
- Sol–gel coating technique is a simple, economic, and effective method to produce high quality coatings.

Due to its ability to produce crystalline films at relatively low temperatures, possibility to tailor the microstructures, and its convenience for complex shape coatings, sol–gel derived coatings are being widely explored to develop CaP coatings on metallic materials for implant applications (Paital & Dahotre, 2009).

3.4 Biomimetic

The word biomimetics originates from Greek “Bios” (life, nature) and “Mimesis” (imitation, copy) and can be defined as “the investigation of the structures and functions of biological materials that allows possible future design and synthesis of engineered composites based on the principles obtained from the biological materials” as cited in (Ak Azem, 2008). Recent research showed that the biomimetic process is one of the most promising techniques for producing new biomaterials at ambient conditions (Li , Feng, Cui, Li, & Schubert, 2002).

Biomimetic techniques used for CaP coating deposition are carried out in simulated body fluids (SBF) in near-physiological conditions, where CaP phases are precipitated out of solution and ‘grown’ on the desired substrate (Shadanbaz & Dias, 2012). This technique allows to coat complex-shaped materials, and to co-precipitate biologically active molecules with apatite crystals onto metal implants (Bigia et al., 2005).

Studies concerned with biomimetic coatings on non-biodegradable materials such as titanium substrates did not consider the effect of immersion time in SBF on substrate corrosion. Previous investigations have indicated that prolonged immersion in SBF will result in as thicker coating formation only if the supply of calcium and phosphate ions is plentiful, i.e. the concentration of the SBF is high enough. In these circumstances, investigators have demonstrated a second immersion in fresh SBF solution to be effective. However, that it would be advantageous to adapt the biomimetic protocol for biodegradable substrates such as Mg by reducing incubation times in SBF, thereby minimizing possible degradation during the coating process (Shadanbaz & Dias, 2012).

3.5 Electrophoretic Deposition

Electrophoretic deposition (EPD) is a colloidal process in ceramic production. It offers easy control of the thickness and morphology of the coating through simple arrangement of the deposition time and applied potential. In EPD, charged powder particles dispersed or suspended in a liquid medium are attracted and deposited onto a conductive substrate of opposite charge on application of a DC electric field as shown in Figure 3.4 (Wong & Kwok, 2008).

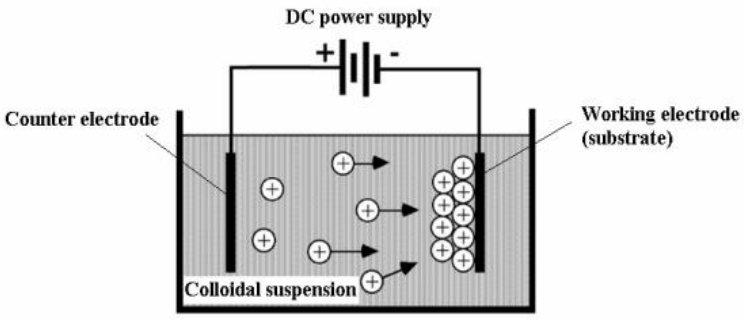

Figure 3.4 Schematic of EPD process.

Nowadays, EPD of calcium phosphate coatings on the metallic implants for biomedical applications is a promising technique. Electrophoresis was chosen for its

outstanding properties such as efficiency, economy and flexibility. Generally, a short deposition time is required for coating (a few seconds to a few minutes) and uniform coatings of complex shapes can be easily formed. With increasing deposition time and voltage, the thickness of the obtained coating increases.

The limitation of EPD is that, the bonding strength between the coating and metal substrates is weak, so post-sintering is required. Heating process has some problems in terms of degradation of the HAP coatings and deterioration of the metal substrates (Wei, Ruys, Milthorpe, Sorrell, & Evans, 2001).

3.6 Electrodeposition

Electrochemical deposition of metals and alloys involves the reduction of metal ions from aqueous, organic, and fused-salt electrolytes. The reduction of metal ions M^{z+} in aqueous solution is represented by;

$$M^{z+}_{solution} + z\text{e} \longrightarrow M_{lattice} \tag{3.1}$$

This can be accomplished by means of two different processes: (1) an electrodeposition process in which *z* electrons (e) are provided by an external power supply, and (2) an electroless (autocatalytic) deposition process in which a reducing agent in the solution is the electron source (no external power supply is involved). These two processes, electrodeposition and electroless deposition, constitute the electrochemical deposition (Paunovic & Schlesinger, 2006).

In the cathodic electrodeposition method, the following reactions that generate OH^- include the reduction of water, dissolved oxygen, nitrate and perchlorate ions (Zhitomirsky, 2002):

$$2H_2O + 2e^- \rightarrow H_2 + 2OH^- \tag{3.2}$$

$$NO_3^- + H_2O + 2e^- \rightarrow NO_2^- + 2OH^- \tag{3.3}$$

$$O_2 + 2H_2O + 4e^- \rightarrow 4OH^- \tag{3.4}$$

$$NO_3^- + 7H_2O + 8e^- \rightarrow NH_4 + 10OH^- \quad (3.5)$$

$$ClO_4^- + H_2O + 2e^- \rightarrow ClO_3^- + 2OH^- \quad (3.6)$$

$$ClO_4^- + 4H_2O + 8e^- \rightarrow Cl^- + 8OH^- \quad (3.7)$$

These reactions consume H_2O to produce OH^- ions, resulting in an appreciable pH increase near the cathode surface. It is important to note that some pH changes take place, even at open circuit, leading to deposit formation (Zhitomirsky, 2000, 2002). When an electrode is immersed in an aqueous solution containing metal ion, the electrode shows the equilibrium potential (E_e). Then, during the electrodeposition at current flow, the different potential (E_{dep}) is measured. The difference between E_e and E_{dep} is called over potential (η) (Caspari, 1899).

The step flow of electrodeposition is basically consists of diffusion of metal ion to the reaction site (1) and electron transfer (2).

When the electron transfer step (2) is slower than the diffusion step (1), electron transfer is the deposition-rate determining step and relationship between η and current density (i), which is corresponding to deposition-rate, is characterized by the Tafel equation as follows (Tafel, 1905) ;

$$\eta = a + b\log|i| \quad (3.8)$$

where a and b are constants. Therefore, in this case, electrodeposition rate is controllable by overpotential η.

On the other hand, when the diffusion step (1) is the deposition-rate determining step, current density (i) is shown in following equation:

$$i = nFD\frac{C}{\delta} \quad (3.9)$$

where n is the number of electrons involved in the reaction, F is the Faraday constant, D is the diffusion coefficient, C is the bulk concentration of metal ion, and δ is the diffusion layer thickness. In this case, electrodeposition rate is controllable

by bulk concentration of metal ion and/or agitation, which will lead to reduce diffusion layer thickness.

An electrolytic cell using in electrochemical deposition shown in Figure 3.5. The working electrode (sample) is the electrode in an electrochemical system on which the reaction of interest is occurring. For corrosion applications, the material of the working electrode is the material under investigation (which is actually corroding). The counter electrode, is an electrode which is used to close the current circuit in the electrochemical cell. It is usually made of an inert material (e.g. Pt, Au, graphite, glassy carbon) and usually it does not participate in the electrochemical reaction. The reference electrode is an electrode which has a stable and well-known electrode potential and it is used as a point of reference in the electrochemical cell for the potential control and measurement (Bard & Faulkner, 2001).

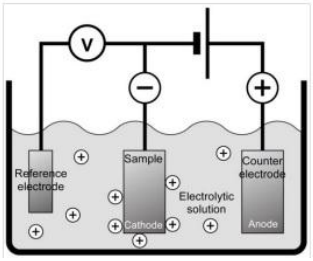

Figure 3.5 Schematic of electrolytic cell using in electrochemical deposition.

It has been suggested electrodeposited systems protecting materials with coatings are composed of following regions:

- The substrate interface,
- The substrate-coating interface,
- The coating,
- The coating-environment interface has to be considered (Holleck, 1986).

Many parameters have effect on these regions. First layer is the substrate where potential hydrogen embrittlement effects are of concern. Cathodic concentration polarization may result in the evolution of hydrogen as the competing reaction. The pH of the cathode film increases and hydrates or hydroxides may precipitate and be

occluded in the deposit. The co-deposition of hydrogen may result in brittleness of the deposit and, by migration and diffusion into the substrate, result in hydrogen embrittlement (Schwartz, 1994). For the substrate-coating interface, adhesion and interdiffusion are of importance. The third region is the coating itself where composition and microstructure determine properties and factors such as stress, phase transformations and grain growth exert noticeable influences. The final zone is the environment interface where the interaction of the coating in its intended application has to be considered in terms of corrosion and wear (Dini, 1993).

Adhesion refers to the bond (chemical or physical) between two adjacent materials, and is related to the force required to effect their complete separation.

Good adhesion is promoted by:

- strong bonding across the interfacial region,
- low stress gradients, either from intrinsic or applied stress,
- absence of easy fracture modes, and
- no long term degradation modes.

Adhesion of a coating to its substrate is critical to its function. Mechanical, chemical, and metallurgical factors may contribute to such adhesion. Good adhesion performance of a coating depends on a variety of the attributes of the interface region, including its atomic bonding structure, its elastic modulus and state of stress, its thickness, purity and fracture toughness.

Diffusion is an irreversible and spontaneous reaction in a system to achieve equilibrium through the elimination of concentration gradients of the atomic species comprising the couple. Atoms or molecules within a material move to new sites and the net movement is from the direction of regions of low concentration in order to achieve homogeneity of the solution, which may be a liquid, solid or gas (Sard, Leidheiser, & Ogbum, 1975). The region near the electrode surface where the concentration of the ions differs from that of the bulk of solution is called the

diffusion or boundary layer. It is defined somewhat arbitrarily as the region where the concentrations differ by 1% or more. The diffusion layer is much thicker than the electrical double layer (approximately 15,000 to 200,000 times thicker, depending on agitation and temperature. Diffusion can result in degradation of the properties of a deposit, particularly at the basis metal interface (Sard, Leidheiser, & Ogbum, 1975). An effective way to minimize or eliminate potential diffusion problems is the use of barrier coatings.

In some instances, diffusion can benefit coating applications. Examples include deposition of alloy coatings and diffusion welding which utilizes diffusion to produce high integrity joints in a range of both similar and dissimilar metals.

The advantages of electrodeposition methods are evident;

- The deposition of thin, not monolithic layers with a composition, crystal size, and chemical history close to that of bone mineral is possible.
- The thickness and chemical composition of coatings can be controlled down to the submicrometer level.
- Generation of coatings with a high specific surface area is possible.
- Compared to the biomimetic method of incubation in simulated body fluid, there is more defined, higher relative supersaturation at the interface, resulting in shorter processing times.
- Owing to possible physiological processing parameters (pH, temperature, aqueous solution), the deposition of calcium phosphate phases can be combined with the immobilization/incorporation of organic components such as proteins (peptides).
- There is no adverse effect of heat on the substrate material.
- It is a low energy process.
- It is a low cost process (with respect to production and waste management).

Hence, electrodeposition of HAP coatings has aroused great interest for biological applications.

The disadvantage of the electrodeposition method is as follow;

- For extreme electrochemical conditions (high current densities, long duration polarization) there is a risk of hydrogen embrittlement for metallic substrates (Scharnweber & Bierbaum, 2009).

CHAPTER FOUR
EXPERIMENTAL STUDY

4.1 Preparation of the Substrate

Ti6Al4V was selected as the substrate material with a diameter of 16 mm. Composition of the Ti6Al4V shown in Table 4.1. Substrates were abraded in series with 80, 240, 400, 800, 1000 and 2000 SiC paper and polished with the 3 μm diamond paste in order to obtain scratch-free mirror-finish surface. The polished specimens were cleaned ultrasonically in deionized water/ethanol mixture for 10 minute, and dried at room temperature.

Table 4.1 Composition of the Ti6Al4V.

Material	**Common standart represantation**	**Chemical composition (% weight)**	
Ti6Al4V	ASTM F136	Ti: 88.3-90.8 Al: 5.5-6.5 V: 3.5-4.5 C: <0.08	H: 0.0125 Fe: <0.25 N: <0.05 O: <0.13

4.2 Deposition of the CaP Coatings

The electrochemical deposition of CaP coatings on Ti6Al4V substrates was conducted in the mixed solution of calcium nitrate tetrahydrate ($Ca(NO_3)_2.2H_2O$, Merck), ammonium dihydrogen phosphate ($NH_4H_2PO_4$, Merck) and distilled water.

Deposition of CaP was carried out by galvanostatic method in a three-electrode cell using Gamry Reference 600 potentiostat–galvanostat. In galvanostatic method, current of the system is held constant, keeping the turnover of the electrochemical reactions at the working and counter electrodes independent of time. Compared to the potentiostatic polarization, the galvanostatic regime results in a stronger increase of the current density over time for surface areas existing for electrochemical

reactions. This can be paid attention to by decreasing the current density during deposition (Scharnweber & Bierbaum, 2009).

An electrochemicall cell is shown in Figure 4.1. Ti6Al4V substrate, graphite plate and saturated calomel electrode were used as working electrode, counter electrode and reference electrode, respectively.

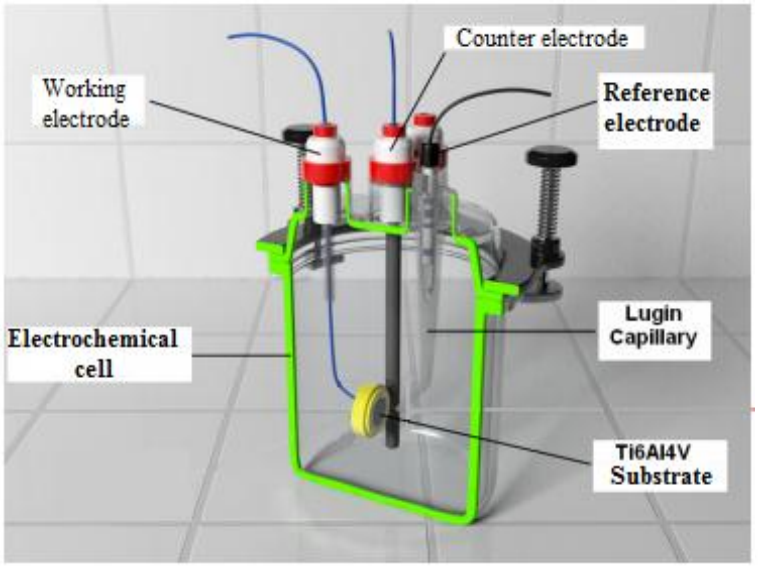

Figure 4.1 Electrochemical cell using for electrochemical deposition.

(Ca + Mg)/P ratio was kept at 1.67 during the preparation of Mg-substituted CaP electrolytes. According to the Mg contents of 0% wt, 10% wt, 20% wt and 40% wt, obtained coatings were named as Mg-0, Mg-1, Mg-2 and Mg-3, respectively. Amount of additive in electrolytes is shown in Table 4.2.

Table 4.2 Amount of additive in electrolytes Mg-0, Mg-1, Mg-2 and Mg-3.

Additives	**Abbrevations**			
	Mg-0	**Mg-1**	**Mg-2**	**Mg-3**
Ca	42 mM	37.8 mM	33.6 mM	25.2 mM
P	25 mM	25 mM	25 mM	25 mM
Mg	-	4.2 mM	8.4 mM	16.8 mM

The electrochemical deposition of Mg-substituted CaP coatings on Ti6Al4V substrates was conducted in the mixed solution of calcium nitrate tetrahydrate

($Ca(NO_3)_2.2H_2O$, Merck), ammonium dihydrogen phosphate ($NH_4H_2PO_4$, Merck), magnesium chloride ($MgCl_2$, Merck) and distilled water. Four different solutions were prepared with different Mg content: Mg-0, Mg-1, Mg-2 and Mg-3. The electrolytes were stirred with a magnetic stirrer at 37 °C for 1 h to enhance the dissolution of components homogenously.

The synthetic sequence used to produce brushite coatings on metallic substrates is a combination of electrochemical half reactions, acid-base reactions, and precipitation reactions. First, water is reduced at the cathode surface to produce hydrogen gas and hydroxide ions, as shown in the following half reaction (Redepenning, Schlessinger, Burnham, Lippiello, & Miyano, 1996):

$$2H_2O + 2e^- \rightarrow H_2 + 2OH^- \quad (4.1)$$

Thus, by controlling the current that passes, the pH is controlled at the surface of the device. The hydroxide ions generated at the surface then may react with dihydrogen phosphate according to the equilibrium shown below:

$$OH^- + H_2P0_4^- \Leftrightarrow H_2O + HP0_4^{2-} \quad (4.2)$$

The following equilibrium for precipitation of, brushite ($CaHPO_4.2H_2O$), is relevant in the presence of calcium ions:

$$Ca^{2+} + HP0_4^{2-} + 2H_20 \Leftrightarrow CaHPO_4.2H_2O \quad (4.3)$$

The Mg-substituted CaP coatings were successfully deposited on Ti6Al4V under -1 mA/cm^2 current density for 1 h. After deposition, the samples were rinsed with distilled water and dried at room temperature.

4.3 Characterization of the Coatings

4.3.1 X-ray Diffraction (XRD)

X-ray diffraction refers to a nondestructive analytical method that uses the diffracted intensity of a monochromatic x-ray beam as a function of the incident and exit angle. Information about the crystallographic structure, chemical composition, and physical properties of materials and thin films can be obtained. In addition, precise lattice parameters, crystallite size, preferred orientation, and lattice stres can be calculate.

When monochromatic x-rays impinge on a sample, the x-rays are scattered (diffracted) by atoms in the material. If the atoms in the material have a crystalline structure, this scattering results in maxima and minima in the diffracted intensity distribution. The signal maxima follow Bragg's law;

$$n.\lambda=2.d.\sin\theta \qquad (4.4)$$

in which n is an integer, λ is the x-ray wavelength, *d* is the distance between crystal lattice planes, and Θ is the diffraction angle. Thus, for each lattice spacing *d*, Bragg's law predicts a maximum at a characteristic diffraction angle Θ. When the intensity of the detected x-rays is plotted as a function of the angle Θ, an XRD pattern is obtained that is characteristic for the sample material (Feddes et al., 2009).

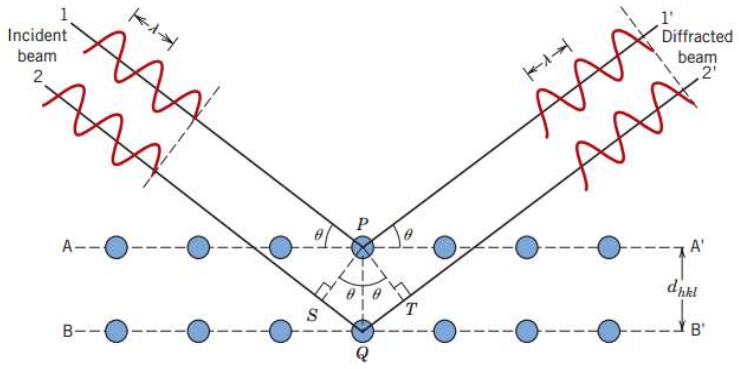

Figure 4.2 Diffraction of x -rays by planes of atoms (A -A ' and B -B ') (Callister, 2007).

In this study coatings were analyzed using X-Ray Diffraction (XRD, Rigaku, D/Max-2200/PC) with a grazing incident angle of 1° at 40 kV and 36 mA using CuK_{α} radiation with a scanning speed of 4° 2θ/min, from 3° to 90°.

4.3.2 Scanning Electron Microscopy (SEM) and Energy Dispersive Spectrum Analyse (EDS)

Scanning electron microscopy (SEM) is one of the most common analytical methods to analyse surface morphology of the solid-state sample. With SEM, an incident electron beam generated by an electron gun, accelerated by high voltage, and focused on the sample surface by a series of electromagnetic lenses scans the surface of the sample by means of a series of deflection coils and synchronized with a cathode-ray tube (CRT). The signals produced as a result of the beam interaction with the sample surface are collected by an suitable detector, amplified, and displayed on the CRT.

The energy dispersive spectroscopy (EDS) is often attached to the SEM. The X-rays generated from the interaction between the electron beam and the sample is used to identify and measure quantitatively the elemental composition of the sample. Therefore, SEM/EDS can specify the elemental composition and obtain the morphology of the sample simultaneously.

In this study, the surface and elemental composition of the films was examined by using JEOL JSM-6060 instrument.

4.3.3 Fourier Transform Infrared Spectroscopy (FTIR)

Fourier Transform Infrared (FTIR or IR) spectroscopy is generally a non-destructive technique, which is used to measure the absorption of various infrared light wavelengths of organic or inorganic materials of interest. The infrared absorption bands specify the specific molecular components or structures, and

provide chemical bonding information of the materials because of the vibrational motions of the chemical bond showing frequencies in the infrared regime.

In this study, chemical composition of the deposited coatings was analyzed by Fourier Transform Infrared Spectroscopy (FTIR, Perkin Elmer Spectrum BX) with a spectral range of 650-4000 cm^{-1} was analyzed.

4.3.4 Electrochemical Method

In this study, the corrosion measurements were carried out using a Gamry potentiostat/galvanostat system controlled by the Gamry Framework software and Echem Analyst software, for the acquisition and analysis of electrochemical data, respectively. Electrochemical characterization was carried out by potentiodynamic measurements in order to measure corrosion performance of the obtained coatings. Corrosion tests were conducted at 36±1°C in simulated body fluid (SBF) solution.

Measurement of the open circuit potentials (OCP) were performed in the test solution for 30 minutes. The potentiodynamic curves were obtained sweeping potential from -1 V vs OCP to 2 V vs SCE at a scan rate of 0.5 mV/s.

4.3.5 Bioactivity Test

Most bone-bonding bioactive materials form bone-like apatite on their surfaces after being implanted into the living body, and bond to neighboring bone through this apatite layer. The apatite layer can be reproduced on the surfaces of materials in an simulated body fluid (SBF) with ion concentrations nearly equal to those of human blood plasma. The bone-bonding ability of a material is often evaluated by investigating the ability of apatite to form on the material in SBF. Therefore, SBF immersion technique was used to evaluate bioactivity of the coatings (Ungan, 2014).

The bioactivity of the coatings was investigated in Kokubo's simulated body fluid (SBF) solution (Kokubo & Takadama, 2006). Order and amounts of the reagents for

preparing 1000 ml SBF was given Table 4.3. The SBF solution was prepared by dissolving reagent-grade chemicals; sodium chloride (NaCl), sodium bicarbonate ($NaHCO_3$), potassium chloride (KCl), dipotassium hydrogen phosphate trihydrate ($K_2HPO_4.3H_2O$), magnesium chloride hexahydrate ($MgCl_2.6H_2O$), calcium chloride ($CaCl_2$) and sodium sulfate (Na_2SO_4) in high purity deionized water and buffered at pH 7.40 with tris-hydroxymethyl-aminomethane ($(CH_2OH)_3CNH_2$) and 1.0 mol/l HCl at 36 ±1.0°C.

Table 4.3 Order and amounts of reagents for preparing 1000ml of SBF.

Order	**Reagent**	**Amount**
1	NaCl	8.035g
2	$NaHCO_3$	0.355g
3	KCl	0.225g
4	$K_2HPO_4.3H_2O$	0.231g
5	$MgCl_2.6H_2O$	0.311g
6	1.0M-HCl	39ml
7	$CaCl_2$	0.292g
8	Na_2SO_4	0.072g
9	Tris ($(HOCH_2)_3CNH_2$)	6.118g
10	1.0M-HCl	0–5ml

Each sample was placed in a polypropylene beaker with 20 ml of SBF and kept in 36±1 °C for 1, 7 and 14 days. To keep the ion concentration stable, the SBF solution was refreshed every 2 days. After immersion samples were taken out from the SBF and gently washed with distilled water and then samples were dried.

CHAPTER FIVE
RESULTS AND DISCUSSIONS

Substitutions (Na^+, K^+, Mg^{2+}, Fe^{2+}, Zn^{2+}, CO_3^{2-}, $Cl^-$and F^-) in the apatite structure play important roles in the biological activity of both bone mineral and CaP-based implant materials.

Magnesium (Mg) is essential for bone metabolism, because the depletion of Mg adversely affects skeletal metabolism and causes the cessation of bone growth. Mg is the fourth most abundant cation in the human body and is thought to interact with osteoblast integrins, which are responsible for cell adhesion and stability (Gopi et al., 2014). Besides, Mg is one of the essential elements for all living organisms, i.e. 60–65% of total amount of Mg in a human body is found in bones and teeth, and the remaining 35–40% of Mg are scattered throughout the rest of the body (Stipniece et al., 2014). Cacciotti et al. (2009), Kolmas et al. (2011) and Kim et al. (2012) reported that presence of Mg incalcified living tissues might improve the biocompatibility and bioactivity of CaP ceramics.

Nowadays, studies on HAP coatings undergo metal ion substitution. Therefore in this study Mg was chosen for substituting element to investigate on bioactivity and corrosion properties of the CaP coatings.

Figure 5.1 shows the XRD patterns of coatings with and without Mg addition named as Mg-0, Mg-1, Mg-2 and Mg-3. For as-deposited coatings the main phases were identified as brushite ($CaHPO_4.2H_2O$, dicalcium phosphate dihydrate) according to JCPDS 072-124 and titanium according to JCPDS 044-1294. The main diffraction peaks were observed at 2Θ (diffraction angle) of 11.52, 21.01, 23.32 and 29.36º each corresponding to brushite ($CaHPO_4.2H_2O$, JCPDS: 072-1240) phase. Additionally, titanium phase was detected at 2Θ of 34.32 and 41.76º representing the Ti6Al4V substrate. Crystallinity degree progressively decreased with increasing Mg content. This results are agreement with the findings of Caciotti et al. (2009).

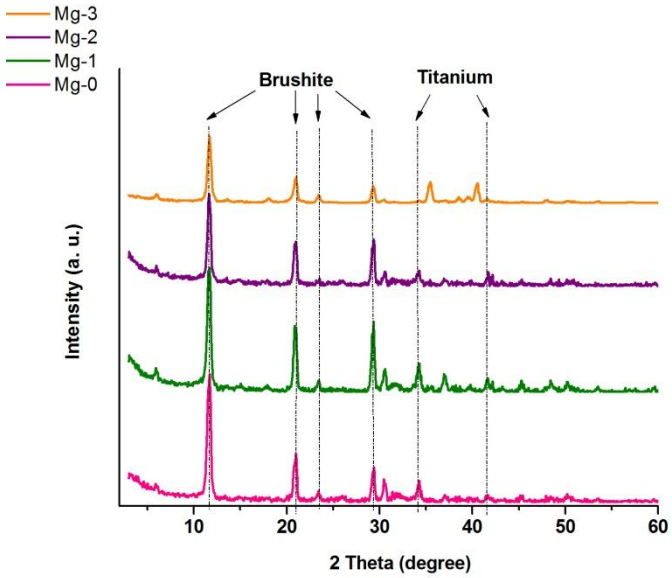

Figure 5.1 XRD patterns of coatings Mg-0, Mg-1, Mg-2 and Mg-3.

Figure 5.2 shows the FTIR spectra of the coatings Mg-0, Mg-1, Mg-2 and Mg-3. The characteristic band at 2360 cm^{-1} due to the HPO_4^{2-} in the brushite (Han, Phillips, & Mikhalovsky, 2008). Band at 1647 cm^{-1} represented the vibration absorbing peak of CO_3^{2-} (Aizawa, Porter, Best, & Bonfield, 2005). Observed vibration mode of carbonate in the FTIR is attributed to the evidence of the precipitated apatite. Also, carbonate ions are part of apatite structures and not as different phase (Shucong, Kithva, Rajendra, Philip, & Khor, 2005). The four sharp distinct bands between 870 $cm^{-}1$ and 1127 cm^{-1} are attributed to the P-O/P-O(H) stretching in both dicalcium phosphates, i.e, DCPD and DCPA (Zhang et al. 2013). The peaks at 784 cm^{-1} was attributed to HPO_4^{2-} (Zhao et al., 2011). The bands observed at 3470 and 3540 cm^{-1} was assigned to O-H stretching and bending of H_2O, due to the moisture in the samples (Zhang et al., 2013). The results showed that broadening and splitting of characteristic absorption band of PO_4^{3-} bands were observed as the Mg content of samples increased. Stipniece et al. (2014) found the similar results in their studies.

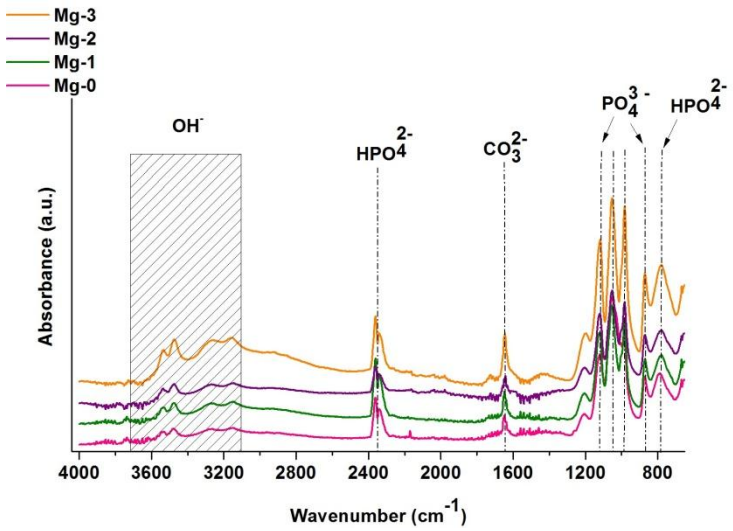

Figure 5.2 FTIR spectras of coatings Mg-0, Mg-1, Mg-2, Mg-3.

Surface morphologies of coatings are presented in Figure 5.3. All coatings indicated a needle-like and plate-like morphology as shown in Figure 5.3. With Mg addition, there is no significant difference in coating morphology. Dimensions of the plate-like and needle-like structures increased with increasing Mg content.

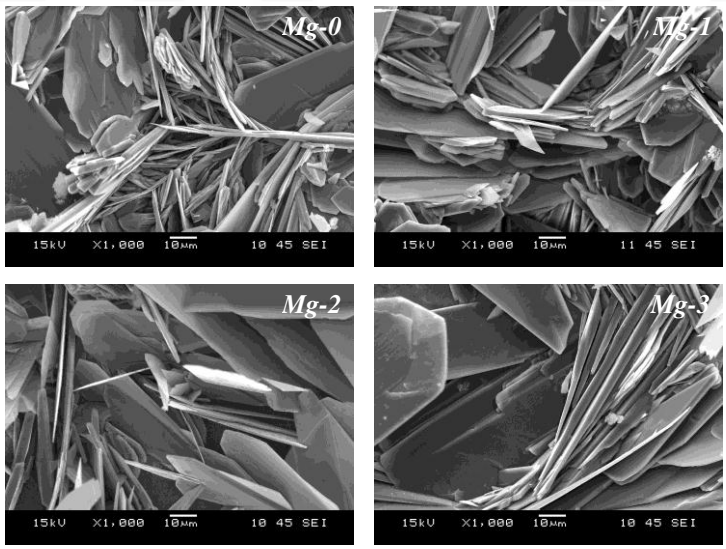

Figure 5.3 Surface morphologies of coatings Mg-0, Mg-1, Mg-2 and Mg-3.

EDS spectrum of the coatings are illustrated in Figure 5.4. Concentration (at %) of the elements and (Ca+Mg):P molar ratios of the as-deposited coatings are given in Table 5.1. Intense peaks for calcium and phosphorous were obtained. Small peaks

corresponding to Ti, Al and V present in the substrate were also detected. These peaks indicate the homogeneous coating structure of the coatings. (Ca+Mg):P ratio of the coatings decreased with increasing Mg ratio. This decreament could be related to substitution of magnesium ions with calcium ions. Cacciotti et al. (2009) found the similar results in their study and it was detected that with increasing Mg rate, (Ca+Mg):P ratio decreased.

Table 5.1 Concentration of the elements in the Mg-0, Mg-1, Mg-2 and Mg-3 coatings.

Element	Concentration (at %)			
	Mg-0	**Mg-1**	**Mg-2**	**Mg-3**
Ca	34.74	43.69	37.11	31.06
P	32.44	33.58	30.53	28.68
O	31.08	21.02	30.57	30.26
Al	0.01	0.01	0.02	0.25
Ti	1.53	1.18	1.48	9.18
V	0.18	0.45	0.20	0.45
Mg	-	0.03	0.07	0.09
(Ca+Mg):P	1.07	1.30	1.21	1.08

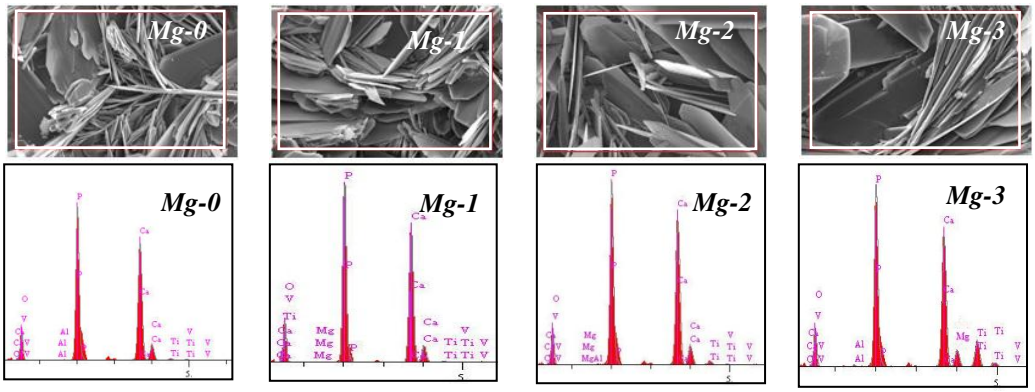

Figure 5.4 EDS spectrum results of coatings Mg-0, Mg-1, Mg-2 and Mg-3.

Potentiodynamic polarization curves from the obtained coating and uncoated Ti6Al4V samples are presented in Figure 5.5. Uncoated Ti6Al4V substrate corrosion properties were investigated in order to compare the effect of coating deposition process incorporation of Mg to CaP compounds.

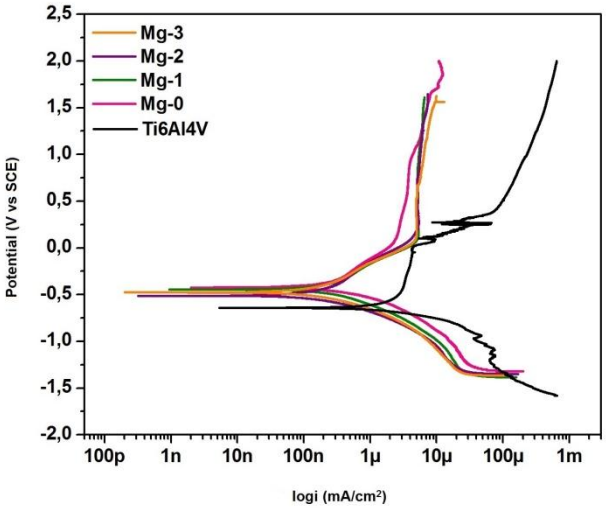

Figure 5.5 Potentiodynamic polarization curves of Mg-0, Mg-1, Mg-2 and Mg-3 coatings.

Electrochemical parameters of the corrosion potential (E_{cor}) and corrosion current density (I_{cor}) were derived from potentiodynamic polarization curves by means of Tafel extrapolation method and results are summarized in Table 5.2. For all of the coatings, E_{cor} generally shifted to noble direction compared to uncoated sample, thus suggesting the improved resistance of the coated Ti6Al4V alloy. Deposition of CaP based coating on Ti6Al4V substrate decreases i_{cor} of the sample from 7.11×10^{-4} mA/cm^2 to 3.29×10^{-4} mA/cm^2. According to the values of I_{cor}, the corrosion resistance of the specimens is ranked as: Mg-0>Mg-1>Mg-3>Mg-2>Ti6Al4V.

According this results, the production of coating on Ti6Al4V substrate improved the protection ability of the substrates, however Mg-substitution did not have a positive effect. The coating with minimum Mg addition possessed the better corrosion properties compared to other coatings with higher Mg addition.

Table 5.2 Electrochemical parameters of the Ti6Al4V substrate and coatings.

Sample	***E_{cor} (mV)***	***I_{cor} (mA/cm^2)***
Mg-0	-368	3.29×10^{-4}
Mg-1	-444	3.04×10^{-4}
Mg-2	-512	2.12×10^{-4}
Mg-3	-475	2.08×10^{-4}
Ti6Al4V	-640	7.11×10^{-4}

According to Cai et al. (2009) results, they found that dissolution occurs faster for coatings with higher Mg content. This is attributed to two possible reasons: the incorporation of Mg into HAP speeds up the dissolution of HAP; the small amount of β-TCMP (Mg-substituted β-TCP) favors the dissolution of the coating due to its higher solubility than Mg-containing HAP. Similarly in this study Mg-substituted brushite coatings showed similar characteristics; with increasing Mg addition corrosion resistance of coatings decreased. Therefore decrement of i_{cor} value of Mg substituted CaP coatings could be explained with similar mechanism.

Surface morphologies of the coatings after corrosion tests are given in Figure 5.6. Dissolution can be observed for all of the coatings. It can be clearly seen that dissolution occurs preferentially in the needle like structure in the coating. Additionally, there is also dissolution process for plate like structures. Dissolution of these structures appear to more for coating Mg-2 by comparison with other coatings.

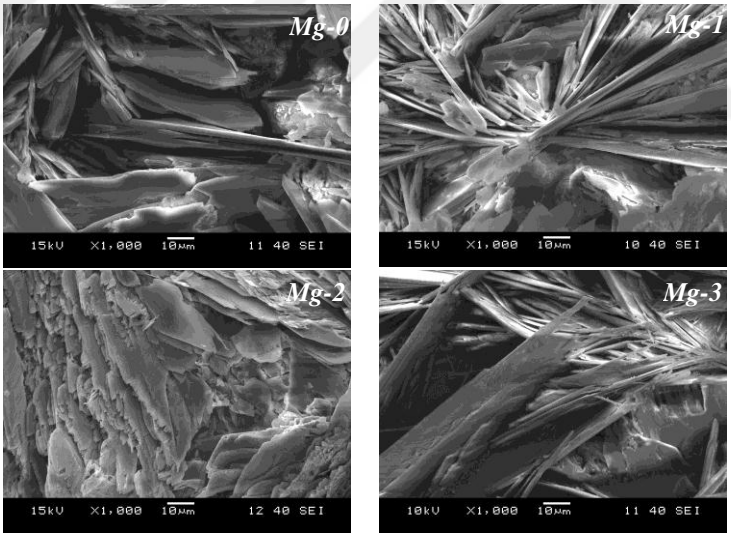

Figure 5.6 Surface morphologies of coatings Mg-0, Mg-1, Mg-2 and Mg-3 after corrosion test.

Figure 5.7 depicts SEM micrograph and EDS spectrum of two different regions of the coating Mg-2. There is some regions where substrate become evident as can be seen from Figure 5.10 (Zone-1). CaP coatings dissolved so much therefore gives low intense EDS peaks for these regions. When spectrums are compared, it can be clearly seen that coating structure degrades more in some regions (Zone 1) in comparision

with other regions (Zone 2). Therefore, EDS peaks of Ti, Al and V elements that represent Ti6Al4V substrate show higher intensity in coating structure.

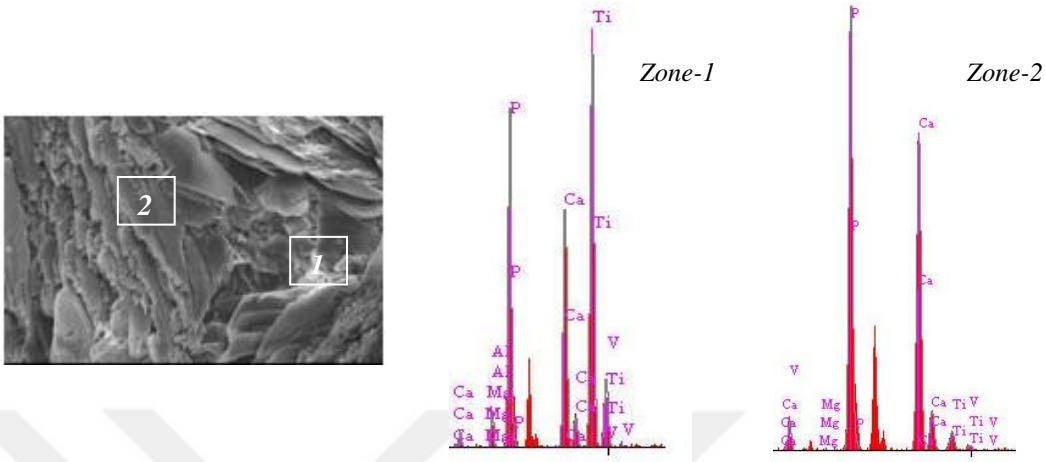

Figure 5.7 EDS results of Mg-2 coating after corrosion tests.

Bioactivity tests of the coatings were performed in SBF solution with varying time 1, 7 and 14 days. Figure 5.8 shows the XRD patterns of the coatings with and without Mg addition after immersion in SBF solution. For as-deposited coatings, the main diffraction peaks were observed at diffraction angle 2Θ of 11.52, 21.01, 23.32 and 29.36º each corresponding to brushite ($CaHPO_4.2H_2O$, JCPDS: 072-1240) phase. Titanium were detected at 2Θ of 34.32 and 41.76º representing substrate. With increasing immersion time, brushite transformed gradually HAP (JCPDS 009-0432) and main phase was identified as HAP. The diffraction peaks were observed at 2Θ (diffraction angle) of 25.88 and 31.86º each corresponding to HAP phase. After 1 day immersion in SBF solution, intensity of brushite phase decreased. HAP phase was identified after 7 day and 14 day immersion.

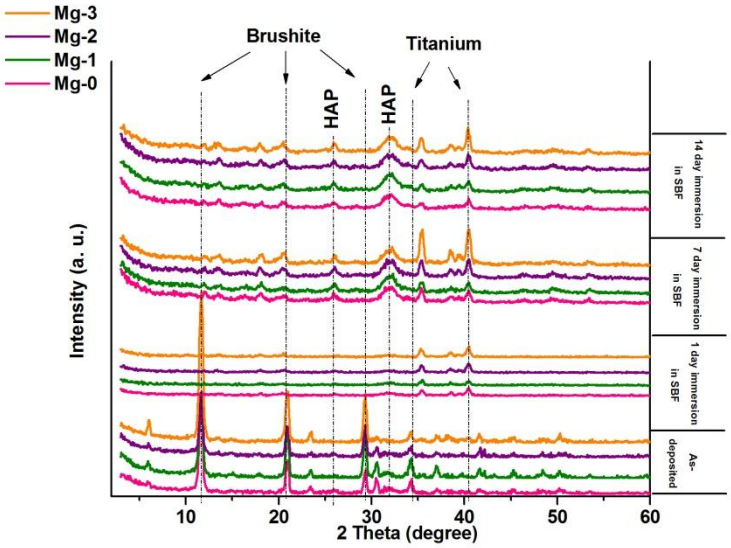

Figure 5.8 XRD patterns of coatings Mg-0, Mg-1, Mg-2 and Mg-3 before and after immersion in SBF.

Figure 5.9 shows the FTIR spectra of the coatings with and without Mg addition after immersion in SBF. It could be seen that PO_4^{3-} absorption peaks (between 870 cm^{-1} and 1127 cm^{-1}) roughly merges and becomes broaden as one peak with increasing immersion time. On the other hand, prolonged immersion time have an adverse effect on intensity of HPO_4^{2-} (784 and 2360 cm^{-1}) bands. This alteration could be interpreted to the phase transformation from DCPD into HAP structure with increasing immersion time in SBF. Absorbed water was showed by the broad bands from 3700 to 3100 cm^{-1}. This may be explained because of the lower crystallinity structure of the coating with increasing immersion in SBF. This result is also in agreement with the XRD findings.

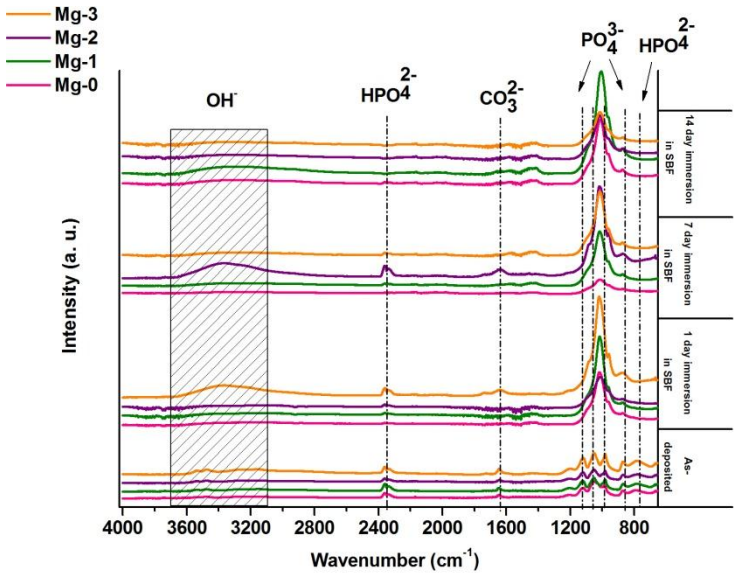

Figure 5.9 FTIR spectras of coatings Mg-0, Mg-1, Mg-2, Mg-3 before and after immersion in SBF.

Figure 5.10 shows surface morphologies of coatings after immersion in SBF. The morphology of the coatings shows an alteration from plate like structure to agglomerated particles and with increasing immersion time size of these particles increase. It could be seen clearly from figures, morphology of the coating surface slightly changed after 1 day immersion in SBF. After 7 days of immersion, samples were fully covered newly grown apatite layer. The morphology of the coating surface transformed to spherical shapes and these spheres completely covered the entire surface. After 14 days of immersion, similar crystals were observed on the coatings surface but coating were more compact and denser which uniformly distributed all over the coating area.

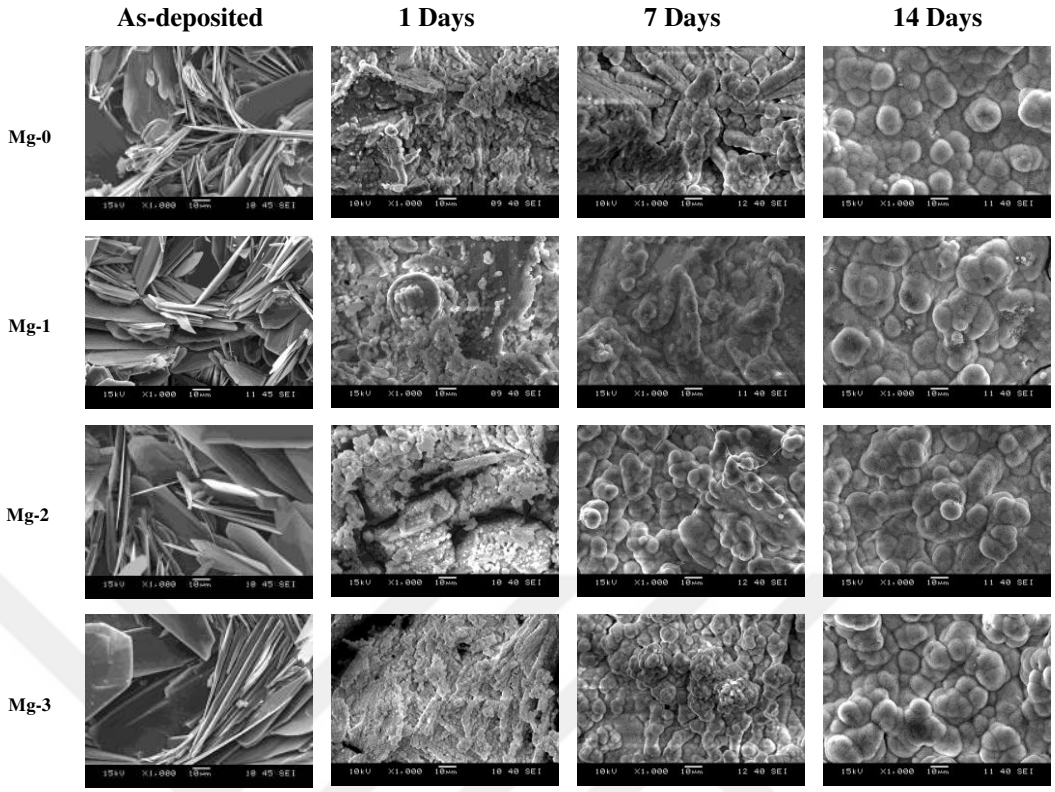

Figure 5.10 Surface morphologies of coatings before and after immersion SBF.

Concentration (at %) of the elements and (Ca+Mg):P molar ratios of the coatings after 1 day, 7 days and 14 days immersion in SBF solution are given in Table 5.3-5.5, respectively. Concentration of calcium increased with immersion in SBF. Thus, (Ca+Mg):P ratios of the coatings increased, as well. Small concentrations corresponding to Ti, Al and V elements present in the substrate were also detected.

Table 5.3 Concentration of the elements in the Mg-0, Mg-1, Mg-2 and Mg-3 coatings after 1 day immersion SBF.

Element	Concentration (at %)			
	Mg-0	**Mg-1**	**Mg-2**	**Mg-3**
Ca	50.90	52.42	42.05	40.90
P	29.76	30.23	23.44	22.54
O	15.68	9.34	14.38	10.31
Al	0.03	1.12	0.38	0.63
Ti	3.36	6.31	18.25	23.90
V	0.24	0.21	0.90	1.00
Mg	-	0.37	0.57	0.69
(Ca+Mg):P	1.71	1.74	1.81	1.84

Table 5.4 Concentration of the elements in the Mg-0, Mg-1, Mg-2 and Mg-3 coatings after 7 days immersion SBF.

Element	Concentration (at %)			
	Mg-0	**Mg-1**	**Mg-2**	**Mg-3**
Ca	53.88	52.62	55.19	56.14
P	26.99	27.39	28.22	26.69
O	18.45	11.99	14.83	15.79
Al	0.03	0.20	0.30	0.19
Ti	0.49	6.06	0.20	0.08
V	0.13	0.86	0.20	0.29
Mg	-	0.85	1.04	0.79
(Ca+Mg):P	1.99	1.95	1.99	2.13

Table 5.5 Concentration of the elements in the Mg-0, Mg-1, Mg-2 and Mg-3 coatings after 14 days immersion SBF.

Element	Concentration (at %)			
	Mg-0	**Mg-1**	**Mg-2**	**Mg-3**
Ca	55.48	53.08	53.69	57.66
P	27.47	27.23	26.95	26.97
O	19.20	17.70	17.47	17.93
Al	0.22	0.20	0.26	0.10
Ti	0.27	0.23	0.23	0.27
V	0.26	0.45	0.39	0.09
Mg	-	1.08	0.98	1.13
(Ca+Mg):P	2.02	1.98	2.02	2.17

CHAPTER SIX
CONCLUSIONS

In this work, productions of Mg-substituted CaP coatings on Ti6Al4V substrate were performed by electrochemical deposition method. Aim of this study was to investigate effects of Mg substitution on structural, corrosion and bioactivity properties of CaP coatings deposited on Ti6Al4V substrates by electrochemical deposition method.

Chemical and morphological characterizations of the coatings were examined by using X-Ray Diffraction (XRD), Fourier Transform Infrared Spectroscopy (FTIR) and Scanning Electron Microscopy (SEM). Additionally, corrosion properties of the coatings were studied electrochemically by potentiodynamic polarization technique in simulated body fluid (SBF) and bioactivity properties of CaP coatings investigated in simulated body fluid (SBF) for varying time periods of 1, 7 and 14 days.

Findings achieved from the experimental works can be summarized as follows:

- According to XRD analyses CaP coating (Mg-0) and Mg-substituted coatings (Mg-1, Mg-2 and Mg-3) are composed of brushite phase. Crystallinity degree of coatings progressively decreased with increasing Mg content.

- Surface morphology of CaP coating (Mg-0) and Mg-substituted coatings (Mg-1, Mg-2 and Mg-3) indicated a needle-like and plate-like structure.

- For all of the Mg-substituted coatings, E_{cor} generally shifted to noble direction compared to uncoated Ti6Al4V substrate. According to the values of i_{cor}, the corrosion resistance of the specimens is ranked as: Mg-0>Mg-1>Mg-3>Mg-2>Ti6Al4V substrate.

- Bioactivity test was done in SBF solution at 36 ±1.0°C. Brushite phase transformed to hydroxyapatite phase completely with immersion in SBF. This results supported by XRD, FTIR and SEM results.

In conclusion, bioactivity properties of the coatings improved with Mg-substitution. On the other hand, there is no affirmative effect of Mg substitution on corrosion properties of the CaP coating.

REFERENCES

Aizawa, M., Porter, A. E., Best, S. M., & Bonfield, W. (2005). Ultrastructural observation of single-crystal apatite fibres. *Biomaterials, 26*, 3427–3433.

Ak Azem, N. F. (2008). *Production of hydroxyapatite coating by sol-gel technique on 316L stainless steel and its corrosion properties*. PhD Thesis, Dokuz Eylül University, İzmir.

Bajpai, P. K., & Fuchs, C. M. (1985). Development of a hydroxyapatite bone grout. In C. W. Hall, (Ed.). *Proceedings of the first annual scientific session of the academy of surgical research* (50–54). New York: Pergamon Press.

Bard, A. J., & Faulkner, L. (2001). *Electrochemical methods–fundamental and applications* (2nd ed.).New York: John Wiley and Sons,.

Barrëre, F., Layrolle, P., Van Blitterswijk, C., & De Groot, K. (2001). Biomimetic coatings on titanium: a crystal growth study of octacalcium phosphate. *Journal of Materials Science: Materials in Medicine, 12(6),* 529–534.

Barrëre, F., van der Valk, C., Dalmeijer, R., Meijer, G., van Blitterswijk, C., de Groot, K., et al. (2003). Osteogenecity of octacalcium phosphate coatings applied on porous metal implants. *Journal of Biomedical Materials Research Part A, 66(4),* 779–788.

Barrëre, F., van Blitterswijk, C., & de Groot, K. (2006). Bone regeneration: molecular and cellular interactions with calcium phosphate ceramics. *International Journal of Nanomedicine, 1(3)*, 317-332.

Bauer, S., Schmuki, P., Klaus von der, M., & Park, J. (2013). Engineering biocompatible implant surfaces Part I: Materials and surfaces. *Progress in Materials Science, 58*, 261-326.

Bigia, A., Boaninia, E. , Braccia, B., Facchinib, A. , Panzavoltaa, S. , Segattib, F., et al. (2005). Nanocrystalline hydroxyapatite coatings on titanium: a new fast biomimetic method. *Biomaterials, 26,* 4085–4089.

Billotte, W. G. (2003). Ceramic Biomaterials. In J. B. Park, & J. D. Bronzino, (Eds.). *Biomaterials principles and applications* (21-55). New York: CRC Press.

Black, J. (1988). Does corrosion matter? *Journal of Bone and Joint Surgery, 70B*, 517–520.

Brauer, G., Szyszka, B., Vergohl, M., & Bandorf, R. (2010). Magnetron sputtering – milestones of 30 years. *Vacuum, 84*, 1354–1359.

Brinker, J. & Scherer, G. (1990). *Sol-gel science: the physics and chemistry of sol-gel processing*. San Diego, CA: Academic Press.

Brunette, D. M., Tengvall, P., Textor, M., & Thomsen, P. (2001). *Titanium in medicine: materials science, surface science, engineering, biological responses and medical applications*. New York: Springer.

Cacciotti, I., Bianco, A., Lombardi, M., & Montanaro, L. (2009). Mg-substituted hydroxyapatite nanopowders: synthesis, thermal stability and sintering behaviour. *Journal of the European Ceramic Society*, 29, 2969–2978.

Cai, Y., Zhang, S., Zeng, X., Wang, Y., Qian, M., & Weng, W. (2009). Improvement of bioactivity with magnesium and fluorine ions incorporated hydroxyapatite coatings via sol–gel deposition on Ti6Al4V alloys. *Thin Solid Films,* 517, 5347–5351.

Callister, W. D. (2007). *Materials science and engineering* (7th ed.). United States of America: John Willey & Sons.

Caspari, W. A. (1899). About electrolytic gas development. *Zeitschrift für Physikalische Chemie, 30,* 89-97.

Dini, J. W. (1993). *Electrodeposition: The materials science of coatings and substrates* (2nd ed.). USA: Noyes Publications.

Disegi, J. A. & Eschbach, L. (2000). Stainless steel in bone surgery. *Injury, 31*, 2-6.

Djoˇsic, M. S., Pani´C, V., Stojanovi´C, J., Mitri´C, M., & Miˇskovi´C-Stankovi´C, V. B. (2012). The effect of applied current density on the surface morphology of deposited calcium phosphate coatings on titanium. *Colloids Surface, A: Physicochemical and Engineering Aspects, 400,* 36-43.

Dowson, D. (1992). Friction and wear of medical implants and prosthetic devices. In P. J. Blau, (Ed.). *ASM handbook v18: Friction, lubrication, and wear technology* (1342-1360). Ohio: ASM International.

Drevet, R., Aaboubi, O., & Benhayoune, H. (2012). In vitro corrosion behavior of electrodeposited calcium phosphate coatings on Ti6Al4V substrates. *Journal of Solid State Electrochemistry, 16,* 3069-3077.

Feddes, B., Gonzalez, P., Serra, J., Pou, J., Chiussi, S., Wolke, J. G. C., et al. (2009). Characterization of Thin Calcium Phosphate Coating. In B. Leon, & J. A. Jansen (Eds.). *Thin calcium phosphate coatings for medical implants* (25-67). New York: Springer.

Feenstra, L. & de Groot, K. 1983. Medical use of calcium phosphate ceramics. In K. De Groot, (Ed.). *Bioceramics of Calcium Phosphate* (131-141). Boca Raton: CRC Press.

Fujishiro, Y., Yabuki, H., Kawamura, K., Sato, T., & Okuwaki, A. (1993). Preparation of needle-like hydroxyapatite by homogeneous precipitation under hydrothermal conditions. *Journal of Chemical Technology and Biotechnology, 57(4),* 349–353.

Gopi, D., Karthika, A., Rajeswari, D., Kavitha, L., Pramod, R., & Dwivedi, J. (2014). Investigation on corrosion protection and mechanical performance of minerals substituted hydroxyapatite coating on HELCDEB-treated titanium using pulsed electrodeposition method. *The Royal Society of Chemistry Advances, 4,* 34751-34759.

Graves, G. A, Hentrich, R. L., Stein, H. G., & Bajpai, P. K. (1972). Resorbable ceramic implants in bioceramics. In C. W. Hall, S. F. Hulbert, S. N. Levine, & F. A. Young, (Eds.). *Engineering and Medicine, Part I* (91–115). New York: Wiley-Interscience.

Habibovic, P., Li, J., van der Valk, C., Meijer, G., Layrolle, P., van Blitterswijk, C. A, & de Groot, K. (2005). Biological performance of uncoated and octacalcium phosphate-coated Ti6Al4V. *Biomaterials, 26(1),* 23–36.

Han, H. M., Phillips, G. J., Mikhalovsky, S. V., FitzGerald, S., & Lloyd, A. W. (2008). Sonoelectrochemical deposition of calcium phosphates on carbon materials: effect of current density. *Journal of Materials Science: Materials in Medicine, 19*, 1787-1791.

Hench, L. L., Interranate, L. V., Caspar, L. A., & Ellis, A. B. (Eds.). (1985). *Inorganic biomaterials. In advances in chemistry series 245: Materials chemistry: An emerging discipline*.Washington DC: American Chemical Society.

Hench, L. L. (1991). Bioceramics: from concept to clinic. *Journal of American Ceramic Society, 74*, 1487-1510.

Hench, L. L. (1998). Bioceramics. *Journal of American Ceramic Society, 81,* 1705-1728.

Hill, D. (1998). *Design engineering of biomaterials for medical devices*. New York: Wiley.

Holleck, H. (1986). Material selection for hard coatings. *The Journal of Vacuum Science and Technology, A4*(6), 2661-2669.

Isa, N. N. C., Mohd, Y., & Yury, N. (2012). Electrochemical deposition and characterization of hydroxyapatite on titanium substrate. *APCBEE Procedia, 3*, 46–52.

Kar, A., Raja, K. S., & Misra, M. (2006). Electrodeposition of hydroxyapatite onto nanotubular TiO_2. *Surface & Coatings Technology, 201*, 3723–3731.

Kelly, P. J. & Arnell, R. D. (2000). Magnetron sputtering: a review of recent developments and applications. *Vacuum, 56*, 159-172.

Khairoun, I., Magne, D., Gauthier, O., Bouler, J., Aguado, E., Daculsi, G., et al. (2002). In vitro characterization and in vivo properties of a carbonated apatite bone cement. *Journal of Biomedical Materials Research Part A, 60(4),* 633–642.

Kim, T. W., Lee, H. S., Kim, D. H., Jin, H. H., Hwang, K. H., Lee, et al. (2012). In situ synthesis of magnesium-substituted biphasic calcium phosphate and in vitro biodegradation. *Materials Research Bulletin, 47,* 2506–2512.

Klein, C. P. A. T., Driessens, A. A., & de Groot, K. (1984). Relationships between the degradation behaviour of calcium phosphate ceramics and their physical chemical characteristics and ultrastructural geometry. *Biomaterials, 5,* 157-160.

Kokubo, T. & Takadama, H. (2006). How useful is SBF in predicting in vivo bone bioactivity? *Biomaterials, 27*, 2907–2915.

Kolmas, J., Jaklewicz, A., Zima, A., Bucko, M., Paszkiewicz, Z., Lis, J., et al. (2011). Incorporation of carbonate and magnesium ions into synthetic hydroxyapatite: the effect on physicochemical properties. *Journal of Molecular Structure, 987,* 40–50.

Kuemmerle, J., Oberle, A., Oechslin, C., Bohner, M., Frei, C., Boecken, I., et al. (2005). Assessment of the suitability of a new brushite calcium phosphate cement for cranioplasty–an experimental study in sheep. *Journal of Cranio-Maxillofacial Surgery, 33(1)*, 37–44.

Kumar, M., Dasarathy, H., & Riley, C. (1999). Electrodeposition of brushite coatings and their transformation to hydroxyapatite in aqueous solutions. *Journal of Biomedical Materials Research Part A, 45(4)*, 302–310.

Kung, K. C., Lee, T. M., & Lui, T. S. (2010). Bioactivity and corrosion properties of novel coatings containing strontium by micro-arc oxidation. *Journal of Alloys and Compounds, 508,* 384-390.

Landi, E., Logroscino, G., Proietti, L., Tampieri, A., Sandri, M., & Sprio, S. (2008). Biomimetic Mg-substituted hydroxyapatite: from synthesis to in vivo behaviour. *Journal of Materials Science: Materials in Medicine, 19,* 239–247.

Lee, H. B., Khang, G., & Lee, J. H. (2003). Polymeric Biomaterials. In J. B. Park, & J. D. Bronzino (Eds.). *Biomaterils Principles and Applications* (55-79). New York: CRC Press.

Leon, B., & Jansen, J. A. (Eds.). (2009). *Thin calcium phosphate coatings for medical implants*. New York: Springer.

Li , F., Feng, Q. L., Cui, F. Z. , Li, H. D. , & Schubert, H. (2002). A simple biomimetic method for calcium phosphate coating. *Surface and Coatings Technology, 154*, 88–93.

Mudali, U. K., Sridhar, T. M., & Raj, B. (2003). Corrosion of bio implants. *Sadhana, 28,* 601-637.

Oonishi, H. (1992). *Bioceramic in orthopaedic surgery—our clinical experiences*. In J. E. Hulbert, & S. F. Hulbert, (Eds.). *Bioceramics, Vol. 3* (31–42). India: Rose Hulman Institute of Technology.

Paital, S. R. & Dahotre, N. B. (2009). Calcium phosphate coatings for bio-implant applications: materials, performance factors, and methodologies. *Materials Science and Engineering:R, 66*, 1–70.

Park, J. B. (1984). *Biomaterials science and engineering*. New York: Plenum Press.

Park, J. & Lakes, R. S. (2007). *Biomaterials:an introduction* (3rd ed.). New York: Springer.

Paunovic, M., & Schlesinger, M. (2006). *Fundamentals of electrochemical deposition*, (2nd ed.). New Jersey: Wiley-Interscience.

Ratner, B. D., Hoffman, A. S., Schoen, F. J., & Lemons, J. E. (2004). *Biomaterials Science* (2nd ed.). New York: Elsevier Academic Press.

Redepenning, J., Schlessinger, T., Burnham, S., Lippiello, L., & Miyano, J. (1996). Characterization of electrolytically prepared brushite and hydroxyapatite coatings on orthopedic alloys *Journal of Biomedical Materials Research*, *30(3)*, 287-294.

Reiner, T., & Gotman, I. (2010). Biomimetic calcium phosphate coating on Ti wires versus flat substrates: structure and mechanism of formation. *Journal of Materials Science: Materials in Medicine, 21(2)*, 515-523.

Sard, R., Leidheiser, H., & Ogbum, F. (1975). *Properties of electrodeposits: their measurement and significance*. USA: The Electrochemical Society Incorporation.

Scharnweber, D. & Bierbaum, S. (2009). Electrochemically Assisted Deposition of Thin CaP Coatings. B. Leon, & J. A. Jansen (Eds.). *Thin calcium phosphate coatings for medical implants* (2nd ed.) (215-263). New York: Springer.

Schwartz, M. (1994). Deposition from aqueous solutions: An overview. In R. F. Bunshah, (Ed.), Handbook of deposition technologies for films and coatings: science, technology and applications (2nd ed.) (506-617). USA: Noyes Publications.

Shadanbaz, S. & Dias, G. J. (2012). Calcium phosphate coatings on magnesium alloys for biomedical applications: a review. *Acta Biomaterialia, 8,* 20–30.

Shucong, Y., Kithva, P. H., Rajendra, K., Philip, C., & Khor, K. A. (2005). In vitro apatite formation and its growth kinetics on hydroxyapatite/polyetheretherketone biocomposites. *Biomaterials, 26,* 2343-2352.

Stipniece, L., Salma-Ancane, K., Borodajenko, N., Sokolova, M., Jakovlevs, D., & Berzina-Cimdina, L. (2014). Characterization of Mg-substituted hydroxyapatite synthesized by wet chemical method. *Ceramics International, 40,* 3261–3267.

Stulajterov, R. & Medveck, L. (2008). Effect of calcium ions on transformation brushite to hydroxyapatite in aqueous solutions. *Colloids and Surfaces A, 316,* 104–109.

Suwanprateeb, J., Suvannapruk, W., & Wasoontararat, K. (2010). Low temperature preparation of calcium phosphate structure via phosphorization of 3D-printed calcium sulfate hemihydrate based material. *Journal of Materials Science: Materials in Medicine, 21(2), 419–429.*

Suzuki, O., Imaizumi, H., Kamakura, S., & Katagiri, T. (2008). Bone regeneration by synthetic octacalcium phosphate and its role in biological mineralization. *Current Medicinal Chemistry, 15(3),* 305–313.

Tafel, J. (1905). Polarization observed during cathodic liberation of hydrogen. *Zeitschrift für Physikalische Chemie, 50*, 641-650.

Tanzer, M., Kantor, S., Rosenthall, L., & Bobyn, J. (2001). Femoral remodeling after porous-coated total hip arthroplasty with and without hydroxyapatite–tricalcium phosphate coating: a prospective randomized trial. *Journal of Arthroplasty, 16(5),* 552–558.

Theiss, F., Apelt, D., Brand, B., Kutter, A., Zlinszky, K., Bohner, M., et al. (2005). Biocompatibility and resorption of a brushite calcium phosphate cement. *Biomaterials, 26(21),* 4383–4394.

Thian, E. S., Huang, J., Best, S. M., Barber, Z. H., & Bonfield, W. (2007). Silicon-substituted hydroxyapatite: the next generation of bioactive coatings. *Materials Science and Engineering C, 27,* 251-256.

Ungan, G. G. (2014). *Characterization of the Mg doped Ca-P compounds electrochemically deposited on MAO modified implant materials*. PhD Thesis, Dokuz Eylül University, İzmir.

Von Recum, A. F. (1999). Handbook of biomaterials evaluation: Scientific, technical and clinical testing of implant materials(2nd ed.). Philadelphia: Taylor & Francis.

Wei, M., Ruys, A. J., Milthorpe, B. K., Sorrell, C. C., & Evans, J. H. (2001). Electrophoretic deposition of hydroxyapatite coatings on metal substrates: a nanoparticulate dual-coating approach. *Journal of Sol-Gel Science and Technology, 21,* 39–48.

Weng, W., Zhang, S., Cheng, K., Qu, H., Du, P., Shen, G., et al. (2003). Sol–gel preparation of bioactive apatite films. *Surface and Coatings Technology, 167,* 292–296.

Williams, D. F. (1981). *Biocompatibility of clinical implant materials* (1st ed.). New York: CRC Press.

Williams, D. F. (1994). Titanium: epitome of biocompatibility or cause for concern. *The Journal of Bone and Joint Surgery, 76-B*, 348-349.

Wong, P. K. & Kwok, C. T. (2008). Corrosion of nano-hydroxyapatite coating on titanium alloy fabricated by electrophoretic deposition. In Jeremy Gilbert (Ed.). *Medical Device Materials IV: Proceedings from the Materials & Processes for Medical Devices Conference 2007* (1st ed.) (213-219). USA: ASM International.

Yamada, S., Heymann, D., Bouler, J., & Daculsi, G. (1997). Osteoclastic resorption of calcium phosphate ceramics with different hydroxyapatite/[beta]-tricalcium phosphate ratios. *Biomaterials, 18(15),* 1037–1041.

Zhang, J., Dai, C., Wei, J., Wen, Z., Zhang, S., & Lin, L. (2013). Calcium phosphate/chitosan composite coating: Effect of different concentrations of Mg^{2+} in the m-SBF on its bioactivity. *Applied Surface Science, 280,* 256-262.

Zhao, X., Hu, T., Li, H., Chen, M., Cao, S., Zhang, L., et al. (2011). Electrochemically assisted co-deposition of calcium phosphate/collagen coatings on carbon/carbon composites. *Applied Surface Science, 257,* 3612–3619.

Zhitomirsky, I. (2000). New developments in electrolytic deposition of ceramic films. *American Ceramic Society Bulletin, 79*(9), 57-63.

Zhitomirsky, I. (2002). Cathodic electrodeposition of ceramic and organoceramic materials: Fundamental aspects. *Advances in Colloid and Interface Science, 97,* 279-317.